



## Original article

## Cell-penetrating peptoids: Introduction of novel cationic side chains



Dominik K. Kölmel<sup>a</sup>, Anna Hörner<sup>a,b</sup>, Franziska Rönicke<sup>c</sup>, Martin Nieger<sup>d</sup>, Ute Schepers<sup>c</sup>, Stefan Bräse<sup>a,c,\*</sup>

<sup>a</sup> Karlsruhe Institute of Technology (KIT), Institute of Organic Chemistry, Fritz-Haber-Weg 6, D-76131 Karlsruhe, Germany

<sup>b</sup> Karlsruhe Institute of Technology (KIT), Light Technology Institute, Engesserstraße 13, D-76131 Karlsruhe, Germany

<sup>c</sup> Karlsruhe Institute of Technology (KIT), Institute of Toxicology and Genetics, Hermann-von-Helmholtz-Platz 1, D-76344 Eggenstein-Leopoldshafen, Germany

<sup>d</sup> University of Helsinki, Laboratory of Inorganic Chemistry, PO Box 55, FIN-00014, Finland

## ARTICLE INFO

## Article history:

Received 7 December 2013

Received in revised form

25 March 2014

Accepted 27 March 2014

Available online 28 March 2014

## Keywords:

Peptoid

Molecular transporter

Spermine

Cellular uptake

HeLa cell

## ABSTRACT

During the last decade peptoid-based molecular transporters have been broadly applied. They are highly valued for their easy synthesis and their superior stability against enzymatic degradation. The special structure of peptoids generally allows introducing a variety of different side chains. Yet, the cationic side chains of cell-penetrating peptoids displayed solely lysine- or arginine-like structures. Thus this report is intended to extend the spectrum of cationic peptoid side chains. Herein, we present novel functional groups, like polyamines, aza-crown ethers, or triphenylphosphonium ions that are introduced into peptoids for the first time. In addition, the obtained peptoids were tested for their cell-penetrating properties.

© 2014 Elsevier Masson SAS. All rights reserved.

## 1. Introduction

Although the concept of molecular transporters is known since the cell-penetrating properties of the HIV-1 Tat protein were discovered in the late 1980s by Green and Loewenstein [1], and independently by Frankel and Pabo [2], there is still an ongoing demand for new transporters. Nowadays, molecular transporters are defined as substances that possess intrinsic cell-penetrating properties and can thus assist in transporting other substances (e.g. drugs or dyes) through the cell membrane. As bioavailability is a crucial criterion for all bioactive molecules, molecular

transporters can be extremely valuable [3]. In practice, the cellular uptake of a molecule with low bioavailability can be mediated by its covalent conjugation with an appropriate molecular transporter [3]. By doing this, the molecular uptake of diverse cargoes into mammalian and even plant cells can be greatly enhanced [4]. To date, a wide variety of cargoes that greatly differ in size and nature, like small molecules, oligonucleotides, peptides/proteins, nanoparticles or quantum dots, were successfully delivered by molecular transporters [3]. Furthermore, it is possible to address different cellular compartments by altering the structure of the molecular transporter [5]. Therefore, molecular transporters are a promising delivery system for targeted drug delivery [6].

Molecular transporters can be built up from numerous different scaffolds. So far the best characterized transporters are the cell-penetrating peptides (CPPs) [7]. Among the most frequently used CPPs are short sequences of the HIV-1 Tat protein [8], derivatives of the homeoprotein from Antennapedia (e.g. penetratin) [9], the protein transportan [10] and oligomers of arginine. [11] Besides those CPPs, peptidomimetics, such as  $\beta$ -peptides [12] or oligo-carbamates [13], have been described that mimic the cell penetrating properties but display higher stability against enzymatic degradation [14]. Despite their structural diversity, they all are mainly amphiphilic and positively charged under physiological

**Abbreviations:** Boc, *tert*-butoxycarbonyl; CPP, cell-penetrating peptide; CPPo, cell-penetrating peptoid; CuAAC, copper(I)-catalyzed azide-alkyne cycloaddition; DIC, *N,N*-diisopropylcarbodiimide; DMF, *N,N*-dimethylformamide;  $\epsilon_{\max}$ , extinction coefficient;  $\Phi_F$ , fluorescence quantum yield; Fmoc, 9H-fluoren-9-ylmethoxycarbonyl; FRET, Förster resonance energy transfer; *H*, brightness; HeLa, human cervix carcinoma; HIV, human immunodeficiency virus; HOBt, 1-hydroxybenzotriazole; HPLC, high performance liquid chromatography;  $\lambda_{\max,abs}$ , absorption maximum;  $\lambda_{\max,em}$ , emission maximum; Ms, mesyl; PBS, phosphate buffered saline; RT, room temperature; siRNA, small interfering ribonucleic acid; SPPS, solid phase peptide synthesis; Tf, triflyl; TFA, trifluoroacetic acid.

\* Corresponding author. Karlsruhe Institute of Technology (KIT), Institute of Organic Chemistry, Fritz-Haber-Weg 6, D-76131 Karlsruhe, Germany.

E-mail address: [braese@kit.edu](mailto:braese@kit.edu) (S. Bräse).

conditions containing extended regions of lysine- or arginine-like residues [12,13,15,16].

Although the cellular uptake mechanism is not yet revealed in all details, the polycationic character is a very important feature of molecular transporters. It is assumed that the positive charges allow the transporters to interact strongly with the negatively charged structures such as the heparane sulfates and the head groups of membrane phospholipids on the extracellular side of the plasma membrane [17,18]. After the adsorption of the transporter the subsequent translocation through the plasma membrane can take place. There are many different and partially contrary hypotheses for this translocation step, which are controversially discussed. Currently, it is anticipated that most CPPs are taken up by endocytosis [19]. But it is very likely that several CPPs utilize other competing uptake pathways, like direct penetration [19,20]. Furthermore, the actual mechanism may change with the experimental conditions [19]. However, independently from the exact mechanism, it is quite noteworthy that the plasma membrane is not significantly damaged during the cellular uptake of such molecular transporters [19].

Another important class of CPP mimetics is the cell penetrating peptoids (CPPos). These CPPos are oligomers of *N*-substituted glycines and thus unnatural regioisomers of the omnipresent peptides (Fig. 1). Like other peptidomimetics, peptoids are highly stable against enzymatic degradation [14]. Therefore peptoids are well suited for biological applications [21]. Unlike peptides, peptoids have an achiral backbone and typically do not form distinct secondary structures as the tertiary backbone amides are no longer able to act as donors for hydrogen bonding. However, it has been shown that it is possible to stabilize complex secondary or tertiary structures, like helices [22], sheets [23], threaded loops [24], ribbons [25], or turns [26], by introducing suitable side chains. So far, CPPos always had a high content of lysine- and/or arginine-like side chains [16,27]. Interestingly, it could be shown that neither the absence of chirality nor the loss of hydrogen bonding along the backbone has a negative influence on the cellular uptake [28]. Up to now, CPPos have been successfully applied to transport many different cargoes, like siRNA [29], photosensitizers [30], diverse fluorescence dyes [31], or lanthanide ions [32].

Peptoids are superior to most other peptidomimetics because they can be easily assembled on solid supports such as Rink amide resin. There are two different but convergent synthetic strategies: the monomer and the submonomer approach (Scheme 1). The monomer approach is based on the established solid phase peptide synthesis (SPPS). During this approach Fmoc-protected glycine derivatives are activated with *N,N*-diisopropylcarbodiimide (DIC) and 1-hydroxybenzotriazole (HOBt) and reacted with the resin [33]. The coupling step is followed by the deprotection of the *N*-terminus. This sequence of coupling glycine derivatives and Fmoc deprotecting can be repeated iteratively to obtain a peptoid with the desired length. Finally, the peptoid can be cleaved from the solid supports with trifluoroacetic acid (TFA).

The second approach for the synthesis of peptoids was originally introduced by Zuckermann et al. in 1992 [34]. During the first step of the submonomer approach, the resin is acylated with bromoacetic acid. Next, a primary amine is added to the resin and a

nucleophilic substitution with the immobilized bromide can take place. Again, those two steps can be repeated until the desired peptoid is build up. The advantage of this method is that various primary amines [35] can be used directly and that there is no need for a temporary protecting group. Therefore, the submonomer method is often considered as the more elegant approach. Although most peptoids are assembled on solid supports, it should be mentioned that the synthesis can be performed in solution as well [36].

Besides their application as CPPos [37], peptoids have been broadly applied [38], e.g. as antimicrobial drugs [39], antifouling polymers [40], and polymer electrolytes [41], for storing of small molecules [42], to complex metal ions [43], to stabilize nanoparticles [44,45] and for positron emission tomography [37].

The focus of this work was to extend the spectrum of cationic peptoid side chains. Since the polycationic character of molecular transporters plays a crucial role in cellular uptake, changing the side chain functionalities might lead to novel CPPos with different uptake properties or even organ specificity in *in vivo* applications. Therefore, one goal was to introduce side chains with multiple amino functions. By doing this, it should be possible to create CPPos with an increased charge density. Furthermore, we introduced side chains that are positively charged without the need of protonation. The respective CPPos were tested for their cellular uptake. In addition we investigated the influence of the novel side chains on the intracellular distribution of the CPPos.

## 2. Results and discussion

### 2.1. Synthesis

During this work we focused on the synthesis of hexameric peptoids, because this length has been approved for CPPos [27,46]. In addition, all peptoids were labeled with rhodamine B at their *N*-terminus [27b] to enable visualization *via* fluorescence microscopy. The obtained peptoids **1–5** are depicted in Fig. 2.

The first aim was to introduce side chains with multiple amino functions. Those structures would be very interesting as they display higher charge density than common CPPos with just one amino (or guanidino) function per side chain. Unfortunately, starting with the commercially available primary amine **6** as a submonomer the coupling yields were too low to allow an efficient peptoids synthesis *via* the submonomer approach. Thus, the respective monomer **10** was built up (Scheme 2). First, primary amine **6** was treated with ethyl bromoacetate to obtain glycine ester **8** in nearly quantitative yield. Next, the ester was saponified and the secondary amine was protected with Fmoc. The resulting monomer **10** was well suited for the synthesis of a hexameric peptoid by using the classical monomer approach (see peptoid **1**, Fig. 2).

To further increase the number of amino functions per side chain, the natural occurring polyamine spermine should be incorporated into a peptoid as well. Hence, tris-Boc-protected spermine **7** was synthesized according to a procedure from Geall et al. [47] But again, primary amine **7** was not suitable for the submonomer approach. Therefore, monomer **11** was built up by the same sequence as for the synthesis of monomer **10** (alkylation with ethyl bromoacetate [48], saponification, and protection of the *N*-terminus with Fmoc). Monomer **11** was used for the synthesis of a hexameric peptoid. However, a mixture of the different homologous peptoids (monomer to hexamer) was obtained with the hexamer (see peptoid **2**, Fig. 2) as the major product, which could be separated from the other homologues by HPLC. Although the coupling yields of monomer **11** were only moderate, the monomer approach was still clearly superior to the submonomer approach.

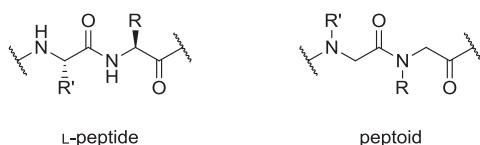
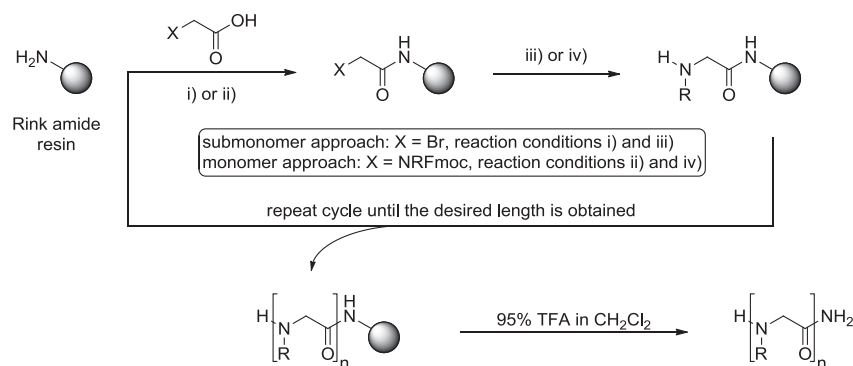
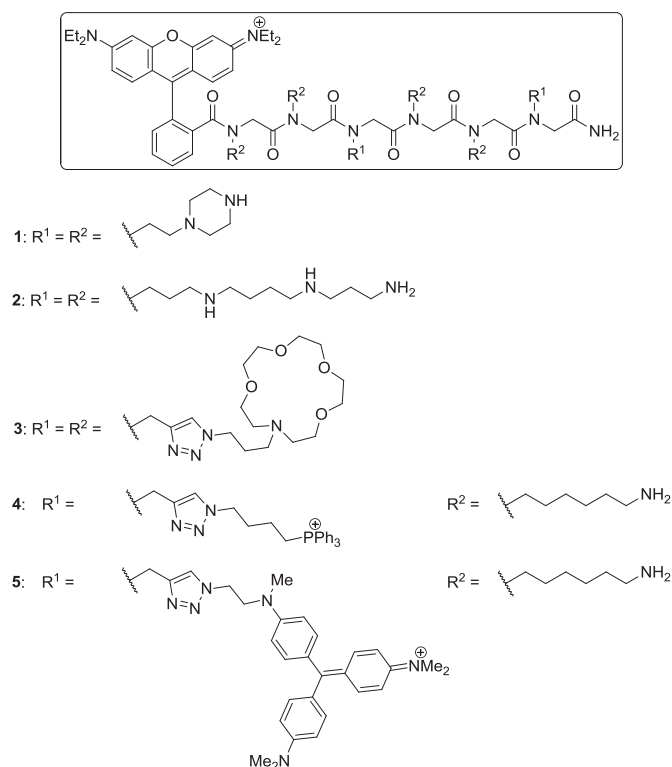


Fig. 1. General structure of the natural occurring L-peptides and peptoids.

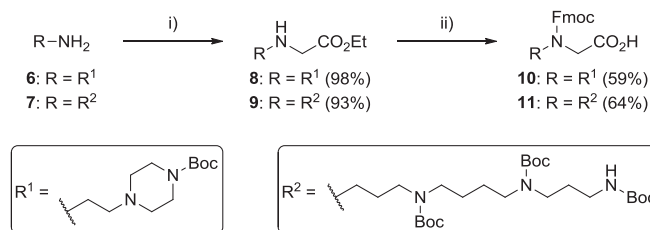


**Scheme 1.** General reaction scheme for the solid phase synthesis of peptoids *via* submonomer [34] or monomer approach. Reagents and conditions: (i) DIC, DMF, RT, 30 min; (ii) DIC, HOBt, DMF, 60 °C ( $\mu$ -wave), 30 min, double coupling; (iii) RNH<sub>2</sub>, DMF, RT, 1 h; (iv) piperidine, DMF, RT, 3 × 5 min.



**Fig. 2.** Structures of the synthesized hexameric peptoids 1–5. In all cases, the *N*-terminus was labeled with rhodamine B.

Besides side chains with multiple amino functions, we also tried other functional groups. The basic idea was to use side chains that do not rely on pH-dependent protonation to provide the required positive charges. One attempt was to use alkali metal ions from the

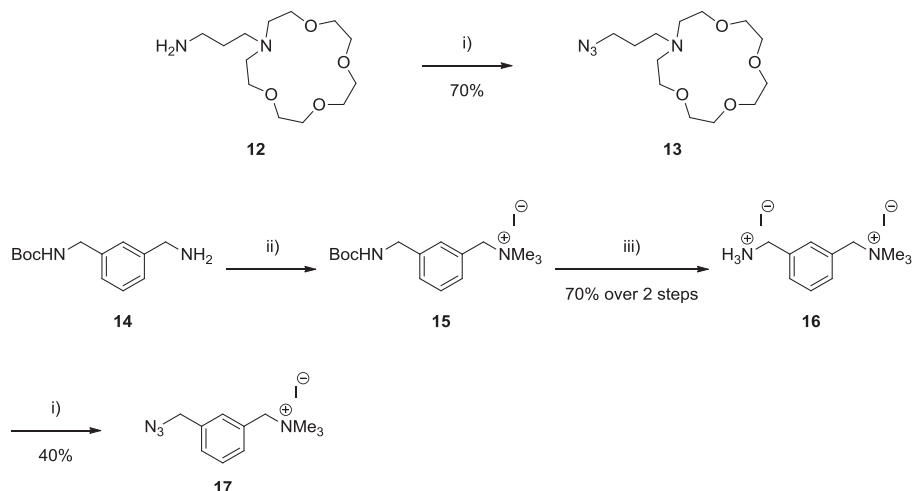


**Scheme 2.** Syntheses of the peptoid monomers **10** and **11**. Reagents and conditions: (i) ethyl bromoacetate, NEt<sub>3</sub>, THF, RT, overnight; (ii) 1) LiOH, dioxane/H<sub>2</sub>O, 0 °C, 3 h; 2) FmocCl, NaHCO<sub>3</sub>, RT, overnight.

extracellular medium to render the peptoids cationic. To achieve this, a crown ether moiety was introduced as a side chain. Initially, *N*-substituted 1-aza-15-crown-5 derivative **12**, which was synthesized according to a procedure of Beer et al., was used as submonomer as such compounds form stable complexes with sodium as well as potassium ions [49,50]. However, the introduction of this novel side chain by submonomer method failed. Therefore, we decided to build up the full length peptoid backbone with subsequent introduction of the crown ether moiety *via* dipolar copper(I)-catalyzed azide-alkyne cycloaddition (CuAAC) [51]. This strategy of postsynthetically modifying side chains by CuAAC was shown to be beneficial for the introduction of various demanding functionalities into peptoids [52]. By using triflyl azide as diazo transfer reagent [53], primary amine **12** could be easily converted into the corresponding azide **13** (Scheme 3). To provide a peptoid with terminal alkynes, propargylamine was used as a submonomer to build up the respective homohexamer (see experimental section). The alkyne side chains could be modified with azide **13** *via* CuAAC. Finally, the peptoid *N*-terminus was labeled with rhodamine B to obtain peptoid **3**.

In addition to the previously discussed side chains, different functionalities bearing intrinsic positive charges were included into peptoids. To produce peptoids with quaternary ammonium ions primary amine **14** was exhaustively methylated (Scheme 3). Eventually, the Boc protecting group of **15** was removed with hydriodic acid. The diiodide **16** could be crystallized from methanol/ethyl acetate. The molecular structure of ammonium ion **16** was determined by X-ray diffraction (Fig. 3). After diazo transfer with TfN<sub>3</sub> azide **17** was obtained in moderate yield. Most notably the preparation of azide **17** did not involve purification by column chromatography as the last two products **16** and **17** can be easily purified by recrystallization. However, the incorporation of azide **17** into peptoids by CuAAC was not successful (data not shown).

Since quaternary ammonium ions could not be introduced into peptoids, we tried to incorporate other charged moieties like phosphonium ions. This would be very interesting, because it is well known that triphenylphosphonium ions can be used for targeting mitochondria [54]. Those lipophilic cations are able to overcome the plasma membrane and the mitochondrial membrane due to the negative transmembrane potential. The triphenylphosphonium moieties were integrated into peptoids by CuAAC. Thus, azide **19** was synthesized according to a procedure of Chen et al. (Scheme 4) [55]. To reduce electrostatic repulsion between the side chains during the modification of the peptoid by CuAAC, Boc-protected aminoethyl residues were used as insulators. This aminoalkyl side chain was chosen, as it has repeatedly proven its effectiveness for cell-penetrating peptoids [16,46]. Hence, the



**Scheme 3.** Syntheses of azides **13** and **17** by diazo transfer with  $\text{TfN}_3$ . Reagents and conditions: (i)  $\text{TfN}_3$ ,  $\text{CuSO}_4$ ,  $\text{K}_2\text{CO}_3$ ,  $\text{MeOH}/\text{H}_2\text{O}$ , RT, overnight; (ii)  $\text{MeI}$ ,  $\text{NaHCO}_3$ ,  $\text{MeOH}$ , RT, 2 d; (iii)  $\text{HI}_{(\text{aq})}$ ,  $\text{H}_2\text{O}$ , RT, overnight.

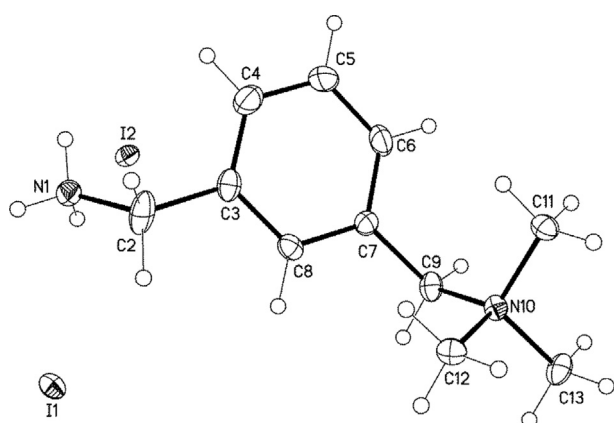
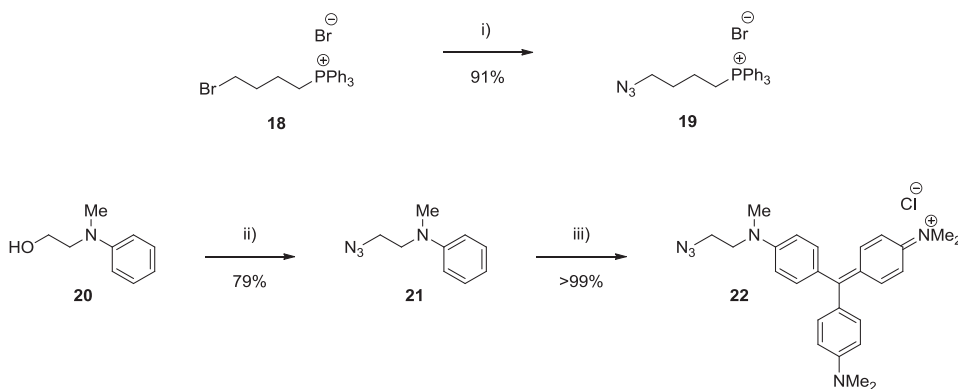


**Fig. 3.** Molecular structure of diiodide **16** with displacement ellipsoids drawn at 50% probability level.

Besides triphenylphosphonium ions, other lipophilic cations such as triarylmethane dyes were conjugated with peptoids. These molecules possess a positive charge that is extensively delocalized and can thus also be applied for targeting mitochondria [56]. To obtain an azide-substituted derivative of the well-known dye crystal violet, azide **21** was synthesized from alcohol **20** (Scheme 4). Finally, azide **21** was reacted with Michler's ketone to obtain the intensively colored triarylmethane dye **22** in quantitative yield. After CuAAC with the same peptoid that was previously used for the incorporation of azide **19**, peptoid **5** (see Fig. 2) could be obtained.

## 2.2. Photophysical characterization

The obtained peptoids **1–5** were spectroscopically characterized to investigate the influence of the novel side chains on the incorporated dye. The compounds were measured in water to facilitate



**Scheme 4.** Syntheses of azides **19** [54] and **22** by nucleophilic substitution with  $\text{NaN}_3$ . Reagents and conditions: (i)  $\text{NaN}_3$ ,  $\text{EtOH}/\text{H}_2\text{O}$ , reflux, overnight; (ii) 1)  $\text{MsCl}$ ,  $\text{NEt}_3$ , RT, 4 h; 2)  $\text{NaN}_3$ ,  $\text{DMF}$ ,  $80^\circ\text{C}$ , 12 h; (iii) 4,4'-bis(dimethylamino)benzophenone,  $\text{POCl}_3$ , toluene,  $100^\circ\text{C}$ , overnight.

obtained peptoid **4** (Fig. 2) comprised two triphenylphosphonium moieties at the first and fourth side chain, which are separated by two aminoethyl residues. The side chains at position five and six were also compromised of aminoethyl residues to diminish the repulsion between the triphenylphosphonium ions and the positively charged dye.

optimal comparability with results from biological tests (Table 1). Besides, peptoid **3** was measured in phosphate buffered saline (PBS) to enable the formation of complexes between the azacrown ethers and sodium ions. In addition, the spectra of rhodamine B were also recorded for comparison. In every case, the spectral maxima of the dye were shifted bathochromically (11–15 nm) upon

**Table 1**  
Spectral properties of rhodamine B-labeled peptoids **1–5**, azide **22** and rhodamine B. If not stated otherwise, all spectra were measured in H<sub>2</sub>O.

Peptoid/Dye	$\lambda_{\max, \text{abs}}$ [nm] <sup>a</sup>	$\epsilon_{\max}$ [M <sup>-1</sup> cm <sup>-1</sup> ] <sup>b</sup>	$\lambda_{\max, \text{em}}$ [nm] <sup>c</sup>	$\Phi_F$
Rhodamine B	554	98,000 ± 3000	575	0.23 ± 0.02
<b>1</b>	567	75,000 ± 3000	587	0.112 ± 0.013
<b>2</b>	567	55,000 ± 2000	586	0.24 ± 0.04
<b>3</b> in PBS	568	98,000 ± 8000	588	0.21 ± 0.06
<b>4</b>	569	53,000 ± 9000	587	0.28 ± 0.03
<b>5</b>	537	90,000 ± 30,000	587	0.0031 ± 0.0003
<b>22</b>	589	52,000 ± 1900	— <sup>d</sup>	— <sup>d</sup>

<sup>a</sup> Absorption maxima have a ±1 nm imprecision.

<sup>b</sup> Calculation is based on the molar mass of the trifluoroacetate salts of the peptoids.

<sup>c</sup> Fluorescence maxima are reproducible within a ±2 nm range.

<sup>d</sup> Could not be determined.

the conjugation with a peptoid. This slight shift is quite typical for various dye–peptoid conjugates [31]. The extinction coefficient was affected by the peptoid as well. In general, the absorption of the conjugates decreased. Nevertheless, the extinction coefficients were still fairly high ( $5.3\text{--}9.8 \times 10^4 \text{ M}^{-1} \text{ cm}^{-1}$ ). The quantum yields of peptoids **2–4** were comparable to the quantum yield of rhodamine B. On the contrary, the quantum yield of peptoid **1** is reduced by half. This finding suggests that the piperazinyl residues of peptoids **1** enable some nonradiative decay ways. Yet, the brightness ( $H = \epsilon_{\max} \times \Phi_F$ ) of the peptoids **1–4** was more than sufficient for biological tests ( $H = 0.8\text{--}2.1 \times 10^4 \text{ M}^{-1} \text{ cm}^{-1}$ ).

Unlike the other peptoids, the spectral properties of transporter **5** were heavily influenced by its side chains. Trityl ion **22** exhibited a strong, broad absorption band in the visible region of the electromagnetic spectrum by itself but did not fluoresce (see Table 1 and Fig. 4). Incidentally, the absorption maximum of triaryl-methane dye **22** (589 nm) matched perfectly with the fluorescence maximum of peptoid-bound rhodamine B (586–588 nm). Therefore, electronic interactions between the trityl ions and the dye of peptoid **5** are very likely. The absorption maximum of peptoid **5** was strongly blue-shifted. Furthermore, peptoid **5** showed just a faint fluorescence. Hence, these trityl side chains have proven to be efficient quenchers if bound to rhodamine B. Such quenching properties are known for crystal violet as well [57]. In this case the quenching could be ascribed to an intramolecular Förster

resonance energy transfer (FRET) [58] between the excited dye and one of the adjacent trityl ions [59].

Principally, FRET is a nonradiative process that is based on long-range dipole–dipole interactions. This energy transfer can always occur if the absorption band of a suitable acceptor is overlapping with the emission band of a donor dye and if the distance between them is not too large (typically 1–10 nm). In the case of peptoid **5** FRET is very likely, as the donor (rhodamine B) and the acceptor (trityl side chain) are in close proximity. The requirement for spectral overlap is fulfilled as well, which can be easily seen by comparing the absorption spectrum of peptoid **5** with the emission spectrum of undisturbed, peptoid-bound rhodamine B (e.g. peptoid **4**, see Fig. 3). Therefore, we concluded that the fluorescence of peptoid **5** is quenched by a highly efficient intramolecular FRET between the excited rhodamine B moiety and the nonfluorescent trityl side chains. Thus, peptoid **5** is only suitable to a limited extent for fluorescence experiments.

### 2.3. Cell tests

The rhodamine B-labeled peptoids **1–5** were tested for their cell-penetrating properties by incubating human cervix carcinoma (HeLa) cells [60] with a 10  $\mu\text{M}$  solution of the respective peptoids. After incubation for 24 h, the peptoids **1–5** could be detected inside the cells *via* live cell fluorescent confocal microscopy (Fig. 5). All peptoids were found to accumulate at least partially in vesicular, most likely endosomal structures, which is quite common for many CPPs [31b,46].

Peptoid **2** was the only CPPo accumulating in the cytosol. Although peptoid **1** had a comparable structure with multiple amino functions, this transporter was not detected in the cytosol but exclusively in vesicles. Moreover, we found that the shorter homologues of peptoid **2** (monomer to tetramer), which were formed as byproducts during the synthesis and could be separated by HPLC, accumulated also entirely in vesicles (data not shown). Thus, we conclude that the cytosol can be targeted if the number of amino groups in the side chains of a peptoid is large enough. The fact that peptoid **2** was found in both the cytosolic and the endosomal compartment led to the assumption that this transporter is released from the endosomes after its initial endosomal uptake. This process is called endosomal escape and there are many examples for the endosomal release of CPPs [61]. For example, it is known that the endosomal escape of CPPs can be triggered by incorporating histidine-rich domains into the peptide. After endocytosis, the imidazolyl residues will become protonated under the acidic conditions of the endosome [62]. This will cause osmotic swelling, which ultimately results in the rupture of the endosome and the release of its content. It is conceivable that a similar mechanism is responsible for the cytosolic localization of peptoid **2**. The degree of protonation of peptoid **2** is likely to increase at the lower pH value of the endosome. As a result peptoid **2** would increase the osmotic pressure of the endosome, which would eventually allow endosomal escape.

The aza-crown ether-containing peptoid **3** was shown to accumulate in vesicles as well. Therefore, the uptake mechanism seems to be comparable to the mechanism of other typical molecular transporters. Apparently, it does not matter how the positive charges are generated (either by protonation or by complexation of alkali metal ions) as long as the transporter is multiply charged under physiological conditions. Surprisingly, the triphenylphosphonium-containing peptoid **4** was also found exclusively in endosomes, although it is known that such phosphonium ions tend to accumulate in mitochondria [54]. Because molecules that are able to target mitochondria are typically lipophilic cations, we think that peptoid **4** is still too polar, mainly due

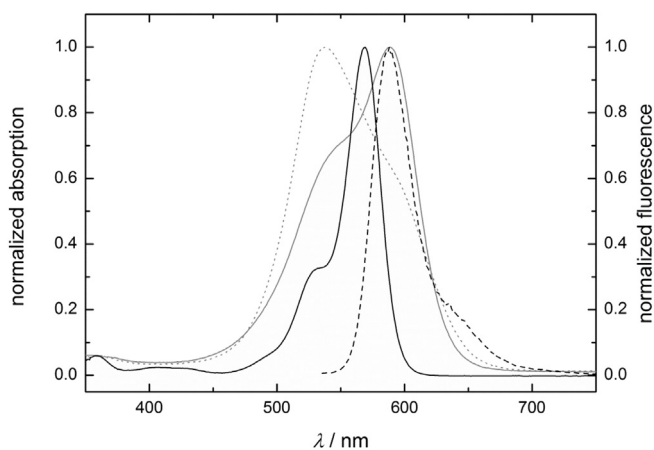


**Fig. 4.** Normalized absorption of peptoids **4** (black) and **5** (gray dotted) and azide **22** (gray). The normalized emission spectrum of peptoid **4** (black dashed) is shown as well. All spectra were recorded in water.

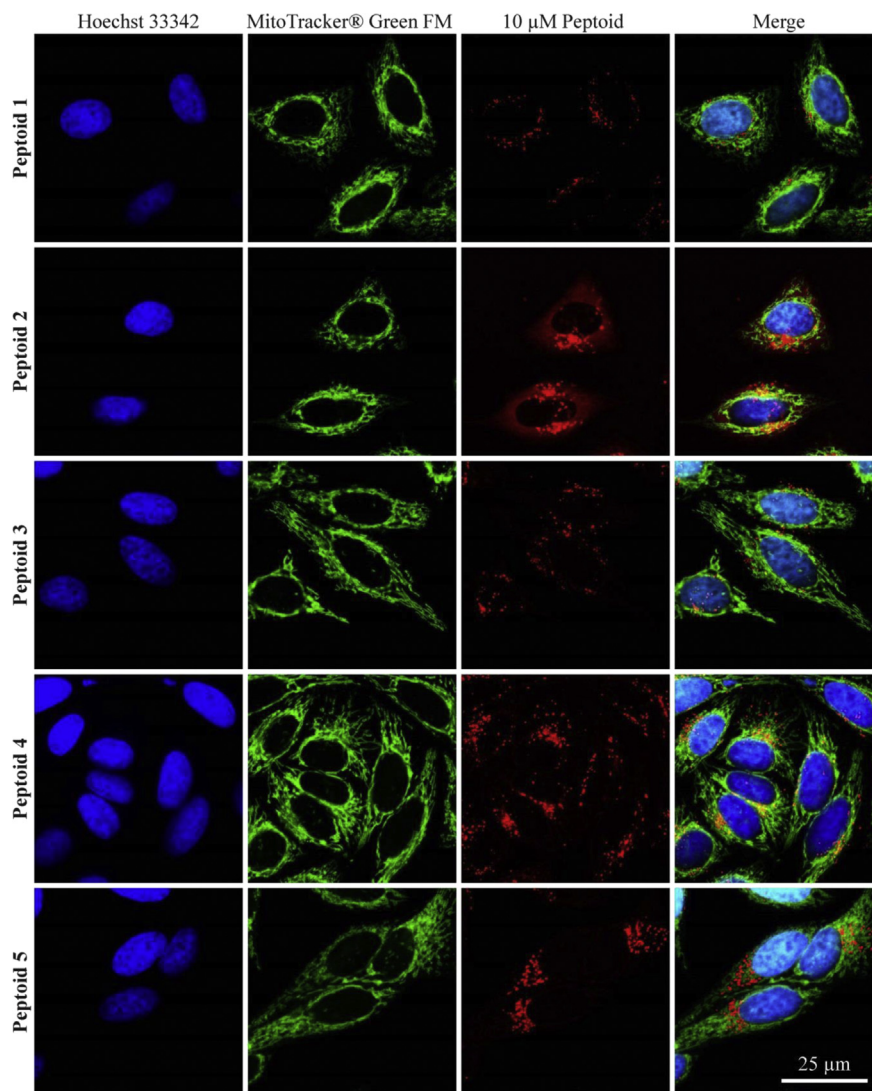


**Fig. 5.** HeLa cells were incubated with a 10  $\mu\text{M}$  peptoid solution for 24 h at 37  $^{\circ}\text{C}$  and subsequently subjected to confocal fluorescence microscopy. To determine the intracellular localization of the peptoids (red), mitochondria were stained with MitoTracker<sup>®</sup> Green FM (green) and nuclei were stained with Hoechst 33342 stain (blue). (For interpretation of the references to color in this figure legend, the reader is referred to the web version of this article.)

to the four aminoalkyl residues. Hence it should be possible to restore the mitochondrial targeting properties by replacing some of the aminoalkyl groups with more lipophilic residues (e.g. benzyl) [37]. Expectedly, peptoid 5 showed just a faint fluorescence signal and only if high laser intensities were applied for the excitation. Besides its vesicular accumulation, this CPPo was also partially localized in mitochondria. Consequently, the triarylmethane dye moieties of peptoid 5 seem to be more lipophilic than the triphenylphosphonium ions of peptoid 4. This is plausible because there are several triarylmethane dyes that were shown to accumulate actively in mitochondria, which is again due to the mitochondrial membrane potential [63]. Nevertheless, triarylmethane dyes are not particularly suitable for molecular transporters, because of their strong fluorescence quenching properties.

### 3. Conclusion

In summary, we presented a set of novel peptoid side chains that can be used for the synthesis of molecular transporters. Among those side chains are piperazinyl and polyamine residues, aza-

crown ethers, triphenylphosphonium ions and triarylmethane dyes. The novel side chains could be introduced into hexameric peptoids either *via* monomer approach or *via* CuAAC. All peptoids were labeled with rhodamine B to allow visualizing their cellular uptake. Despite the fact that all peptoids were taken up by HeLa cells, their intracellular distribution differed in some cases significantly. Peptoids 1 and 3–5 aggregated mainly in vesicular, most likely endosomal structures whereas peptoid 2 was shown to accumulate in the cytosol. The main feature of peptoid 2 is its highly polar structure with multiple amino functions. We assume that those amino functions are required to overcome the endosomal entrapment, which was observed for the other less polar peptoids. In addition, we could show that mitochondria could be targeted as well by introducing lipophilic cations into peptoid 5. However, the triarylmethane dye side chains of peptoid 5 had strong fluorescence quenching properties and thus hamper the applicability of such CPPos. Instead we recommend using triphenylphosphonium ions, like those of transporter 4, which should be more suitable to generate mitochondria targeting peptoids. In conclusion, we think that such cell-penetrating peptoids, which are

capable of targeting specific cell organelles, are very promising, e.g. for manipulating cells or for drug delivery. Hence we plan to investigate the influence of different side chains on the intracellular distribution of peptoid transporters in more detail in the future.

## 4. Experimental protocols

### 4.1. General remarks

UV/vis absorption spectra were recorded by using a Varian Cary 300 scan UV/vis spectrophotometer and fluorescence spectra were recorded by using a Varian Cary Eclipse fluorescence spectrometer. Closed quartz cuvettes with a 1 cm path length were used in all experiments. Fluorescence quantum yield measurements were performed on the previously mentioned fluorometer and UV/vis instrument. The slit width was 5 nm for both excitation and emission. Relative quantum efficiencies were obtained by comparing the absorption values and the areas under the emission spectrum for the unknown substance with a standard (rhodamine B in water,  $\Phi_F = 0.23$ ) [64]. The following equation was used to calculate quantum yields:

$$\Phi_x = \Phi_s \times (F_x/F_s) \times (n_x/n_s)^2 \times (A_s/A_x)$$

$\Phi_s$  is the reported quantum yield of the standard,  $F$  is the integrated emission spectrum,  $A$  is the absorbance at the extinction wavelength, and  $n$  is the refractive index of the solvents used. The subscript  $x$  denotes unknown and  $s$  denotes standard. All reactions were carried out under stirring. Reactions under inert gas were carried out in flasks equipped with septa under argon (supplied by using a standard manifold with vacuum and argon lines). Analytical TLC was performed on MERCK ready-to-use plates with silica gel 60 (F254). Column chromatography: MERCK silica gel 60, 0.04–0.063 mm. For microwave assisted peptoid synthesis the single mode CEM Discover microwave was used. IR spectra were recorded by using Bruker ALPHA-T spectrometer. The samples were measured as films between KBr plates or by using the attenuated total reflection (ATR) technique. The transmission intensities are described as follows:  $s$  = strong (11–40%),  $m$  = middle (41–70%),  $w$  = weak (71–90%),  $vw$  = very weak (91–100%). NMR spectra were recorded at 25 °C by using Bruker Avance 300 (300 ( $^1\text{H}$ ) and 75 MHz ( $^{13}\text{C}$ )), Bruker AM 400 (400 ( $^1\text{H}$ ) and 100 MHz ( $^{13}\text{C}$ )) and Bruker DRX 500 (500 ( $^1\text{H}$ ) and 125 MHz ( $^{13}\text{C}$ )) spectrometer. All spectra are referenced to tetramethylsilane as standard ( $\delta = 0$  ppm) by using the signals of the solvent:

$\text{CDCl}_3$  : 7.26 ppm( $\text{CHCl}_3$ ) or 77.0 ppm( $^{13}\text{CDCl}_3$ )

$\text{CD}_3\text{OD}$  : 3.31 ppm( $\text{CHD}_2\text{OD}$ ) or 49.1 ppm( $^{13}\text{CD}_3\text{OD}$ )

Multiplicities of the signals are described as follows:  $s$  = singlet,  $d$  = doublet,  $t$  = triplet,  $q$  = quartet,  $quin$  = quintet,  $m$  = multiplet,  $m_c$  = centered multiplet. Coupling constants ( $J$ ) are given in Hz. Multiplicities in the  $^{13}\text{C}$  NMR spectra were determined by DEPT (distortionless enhancement by polarization transfer) measurements. Mass spectra (EI or FAB) were obtained by using a Finnigan MAT 90 spectrometer. MALDI-TOF mass spectra of the peptoids were obtained by using a Bruker Biflex IV spectrometer with a pulsed ultraviolet nitrogen laser, 200  $\mu\text{J}$  at 337 nm and a time-of-flight mass analyzer with a 125 cm linear flight path. Reversed phase analytical HPLC was performed using Agilent Series 1100, equipped with a C18 PerfectSil Target (MZ Analytik, 3–5  $\mu\text{m}$ , 4.0  $\times$  250 mm). Flow rate: 1 mL/min; solvent A: 0.1% TFA in water; solvent B: 0.1% TFA in acetonitrile. Reversed phase preparative HPLC was performed using Jasko LC-NetII/ADC Series, equipped

with a C18 Vydac 218TP Series (Grace Davison Discovery Sciences, 5  $\mu\text{m}$ , 22  $\times$  250 mm). Flow rate: 15 mL/min; solvent A: 0.1% TFA in water; solvent B: 0.1% TFA in acetonitrile.

### 4.2. Cell culture techniques for mammalian cells

All procedures with mammalian cells were carried out under sterile conditions.  $1 \times 10^4$  HeLa (human cervix carcinoma) cells were plated into each well of an 8-well  $\mu$ -slide from IBIDI (Ibittreat), Germany, and cultured in 200  $\mu\text{L}$  of Dulbecco's modified Eagle's medium, high glucose (DMEM, Sigma Taufkirchen), supplemented with 10% fetal calf serum (FCS, PAA), and 1 U/mL Penicillin/Streptomycin at 37 °C, 5%  $\text{CO}_2$ .

### 4.3. Treatment of HeLa cells with the rhodamine B-labeled peptoids

The peptoids were dissolved in bidistilled water to yield a 2 mM stock solution and were further diluted with 10% DMEM to yield the respective incubation media. The cells cultured as described above were incubated with the different peptoids at final concentrations of 10  $\mu\text{M}$ . Cellular uptake of the peptoids was measured by live cell confocal fluorescence microscopy in DMEM after 24 h as fixation would alter the intracellular distribution as described for other polycationic species [65].

### 4.4. Subcellular localization

For the intracellular localization of the peptoids, the cells were counterstained with fluorescent markers for different organelles (Molecular Probes, Germany). For mitochondria labeling the cells were treated with 125 nM MitoTracker<sup>®</sup> Green FM for 15 min, according to the manufacturer's manual, and washed three times with PBS. For the staining of the nuclei, the cells were eventually treated with Hoechst 33342 dye (2  $\mu\text{g}/\text{mL}$ ) according to the manufacturer's instructions. The cells were covered with DMEM and subjected to live confocal microscopy at 37 °C and 5%  $\text{CO}_2$  atmosphere.

### 4.5. Live imaging by confocal microscopy

Simultaneous visualization of the colocalization of the peptoids and mitochondria and nuclei was achieved by confocal microscopy using Leica TCS-SP5 II, equipped with a DMI6000 microscope. MitoTracker<sup>®</sup> Green FM was excited using the 488 nm line of an argon ion laser, the nuclei were excited with a UV laser at 364 nm, and the peptoids were excited at 561 nm using a DPSS laser. The objective was a HCX PL APO CS 63.0x1.2 Water UV. The exposure was set to minimize oversaturated pixels in the final images. Fluorescence emission was measured at 417–468 nm (for Hoechst 33342), 499–552 nm (for MitoTracker Green FM) and 593–696 nm (for the peptoids) using simultaneous detection. Image acquisition was conducted at a lateral resolution of 1024  $\times$  1024 pixels and 8 bit depth using LAS-AF 2.0.2.4647 acquisition software.

### 4.6. Chemical synthesis

#### 4.6.1. tert-Butyl 4-(2-((2-ethoxy-2-oxoethyl)amino)ethyl)piperazine-1-carboxylate (**8**)

Ethyl bromoacetate (2.41 mL, 21.8 mmol) was dissolved in THF (55 mL) and added dropwise over 3 h to a stirred solution of compound **6** (5.00 g, 21.8 mmol) and  $\text{NEt}_3$  (9.07 mL, 65.4 mmol) in THF (85 mL). After stirring overnight at RT, the solvent was removed under reduced pressure. The residue was dissolved in water (30 mL) and the product was extracted with  $\text{CH}_2\text{Cl}_2$  (4  $\times$  30 mL). The combined organic layers were washed with water

(2 × 30 mL) and brine (30 mL), dried over Na<sub>2</sub>SO<sub>4</sub>, and evaporated. The product was obtained as colorless oil: yield 6.74 g (98%). IR (KBr):  $\tilde{\nu}$  (cm<sup>-1</sup>) = 3331 (w), 2977 (m), 2935 (m), 2814 (w), 1738 (m), 1698 (s), 1459 (m), 1421 (m), 1366 (m), 1290 (m), 1245 (m), 1173 (s), 1129 (m), 1027 (m), 1005 (w), 987 (w), 929 (w), 866 (m), 769 (w), 574 (vw), 462 (vw); <sup>1</sup>H NMR (500 MHz, CDCl<sub>3</sub>):  $\delta$  (ppm) = 1.28 (t, <sup>3</sup>J = 7.2 Hz, 3H, CH<sub>2</sub>CH<sub>3</sub>), 1.45 (s, 9H, C(CH<sub>3</sub>)<sub>3</sub>), 2.42–2.48 (m, 4H, 2 × CH<sub>2</sub>), 2.55 (t, <sup>3</sup>J = 5.9 Hz, 2H, CH<sub>2</sub>), 2.76 (t, <sup>3</sup>J = 5.9 Hz, 2H, CH<sub>2</sub>), 3.43–3.49 (m, 6H, 3 × CH<sub>2</sub>), 4.19 (q, <sup>3</sup>J = 7.2 Hz, 2H, CH<sub>2</sub>CH<sub>3</sub>); <sup>13</sup>C NMR (125 MHz, CDCl<sub>3</sub>):  $\delta$  (ppm) = 14.2 (CH<sub>3</sub>), 28.4 (CH<sub>3</sub>), 45.5 (CH<sub>2</sub>), 50.5 (CH<sub>2</sub>), 52.8 (CH<sub>2</sub>), 57.5 (CH<sub>2</sub>), 60.9 (CH<sub>2</sub>), 79.7 (C), 154.7 (CO), 172.1 (CO); EI MS:  $m/z$  (%) = 315 (2) [M]<sup>+</sup>, 242 (2) [M–C<sub>3</sub>H<sub>5</sub>O<sub>2</sub>]<sup>+</sup>, 199 (4) [M–C<sub>5</sub>H<sub>10</sub>NO<sub>2</sub>]<sup>+</sup>, 143 (9) [M–C<sub>8</sub>H<sub>16</sub>N<sub>2</sub>O<sub>2</sub>]<sup>+</sup>, 84 (99) [M–C<sub>11</sub>H<sub>21</sub>NO<sub>4</sub>]<sup>+</sup>, 49 (100) [M–C<sub>14</sub>H<sub>24</sub>N<sub>3</sub>O<sub>2</sub>]<sup>+</sup>; HRMS  $m/z$  calc for C<sub>15</sub>H<sub>29</sub>N<sub>3</sub>O<sub>4</sub>: 315.2158; found: 315.2156 [M]<sup>+</sup>.

#### 4.6.2. Ethyl 9,14-bis(tert-butoxycarbonyl)-2,2-dimethyl-4-oxo-3-oxa-5,9,14,18-tetrazaicosan-20-oate (**9**)

The preparation and properties of compound **9** have been reported in Ref. [47].

#### 4.6.3. General procedure for the synthesis of compounds **10** and **11**

LiOH (1.5 equiv., 2 M in H<sub>2</sub>O) was dissolved in water and added to a solution of secondary amine **8** or **9** (1 equiv., 0.5 M in dioxane) in dioxane. The mixture was stirred for 5 h at 0 °C. Afterwards, NaHCO<sub>3</sub> (1.5 equiv.) and FmocCl (1.5 equiv.) were added and the solution was stirred overnight at RT. Next, citric acid (20 mL, 20% in H<sub>2</sub>O) was added and the product was extracted with ethyl acetate (3 × 40 mL). The combined organic layers were washed with brine (20 mL) and the solvent was removed under reduced pressure. The crude product was purified by using column chromatography.

4.6.3.1. 2-(((9H-Fluoren-9-yl)methoxy)carbonyl)(2-(4-(tert-butoxycarbonyl)piperazin-1-yl)ethyl)amino)acetic acid (**10**). After purification (chromatography with eluent EtOAc → MeOH) the title compound was obtained as an off-white solid: yield 6.13 g (59%). Mp 73 °C; IR (ATR):  $\tilde{\nu}$  (cm<sup>-1</sup>) = 3434 (w), 2974 (vw), 1687 (m), 1595 (w), 1477 (w), 1449 (w), 1420 (w), 1364 (w), 1243 (w), 1149 (w), 1047 (w), 1001 (w), 977 (w), 863 (vw), 759 (w), 739 (w), 620 (vw), 540 (vw), 426 (vw); <sup>1</sup>H NMR (300 MHz, CD<sub>3</sub>OD):  $\delta$  (ppm) = 1.49 (s, 9H, C(CH<sub>3</sub>)<sub>3</sub>), 2.19–2.32 (m, 4H, 2 × CH<sub>2</sub>), 2.79–2.92 (m, 2H, CH<sub>2</sub>), 3.06 (t, <sup>3</sup>J = 6.4 Hz, 2H, CH<sub>2</sub>), 3.34–3.68 (m, 4H, 2 × CH<sub>2</sub>), 3.73 (s, 2H, CH<sub>2</sub>), 4.20–4.24 (m, 1H, CHCH<sub>2</sub>), 4.28–4.34 (m, 1H, CHCH<sub>2</sub>), 4.66–4.74 (m, 1H, CHCH<sub>2</sub>), 7.26–7.42 (m, 4H, 4 × CH<sub>ar</sub>), 7.61–7.73 (m, 2H, 2 × CH<sub>ar</sub>), 7.77–7.82 (m, 2H, 2 × CH<sub>ar</sub>), mixture of two rotamers; <sup>13</sup>C NMR (75 MHz, CD<sub>3</sub>OD):  $\delta$  (ppm) = 28.7 (CH<sub>3</sub>), 45.6 (CH<sub>2</sub>), 48.6 (CH), 52.5 (CH<sub>2</sub>), 53.4 (CH<sub>2</sub>), 53.7 (CH<sub>2</sub>), 56.5 (CH<sub>2</sub>), 69.5 (CH<sub>2</sub>), 81.7 (C), 121.1 (CH<sub>ar</sub>), 125.7 (CH<sub>ar</sub>), 128.4 (CH<sub>ar</sub>), 128.8 (CH<sub>ar</sub>), 142.8 (C<sub>ar</sub>), 145.5 (C<sub>ar</sub>), 156.0 (CO), 158.2 (CO), 177.6 (CO), mixture of two rotamers; FAB MS:  $m/z$  (%) = 532 (12) [M+Na]<sup>+</sup>, 510 (8) [M+H]<sup>+</sup>, 408 (9) [M–C<sub>5</sub>H<sub>9</sub>O<sub>2</sub>]<sup>+</sup>, 199 (14) [M–C<sub>18</sub>H<sub>16</sub>NO<sub>4</sub>]<sup>+</sup>, 179 (100) [M–C<sub>14</sub>H<sub>24</sub>N<sub>3</sub>O<sub>6</sub>]<sup>+</sup>, 143 (55) [M–C<sub>21</sub>H<sub>22</sub>N<sub>2</sub>O<sub>4</sub>]<sup>+</sup>, 99 (26) [M–C<sub>23</sub>H<sub>24</sub>NO<sub>6</sub>]<sup>+</sup>; HRMS  $m/z$  calc for C<sub>28</sub>H<sub>36</sub>N<sub>3</sub>O<sub>6</sub>: 510.2604; found: 510.2600 [M+H]<sup>+</sup>.

4.6.3.2. 18-(((9H-Fluoren-9-yl)methoxy)carbonyl)-9,14-bis(tert-butoxycarbonyl)-2,2-dimethyl-4-oxo-3-oxa-5,9,14,18-tetrazaicosan-20-oic acid (**11**). After purification (chromatography with eluent cyclohexane/EtOAc 3:1 → MeOH) the title compound was obtained as a white solid: yield 3.73 g (64%). Mp 70 °C; IR (ATR):  $\tilde{\nu}$  (cm<sup>-1</sup>) = 3367 (vw), 2973 (w), 2930 (w), 1676 (m), 1604 (w), 1478 (w), 1449 (w), 1417 (w), 1364 (w), 1245 (w), 1158 (m), 1072 (w), 999 (w), 866 (w), 759 (w), 740 (w), 670 (vw), 621 (vw), 543 (vw), 493 (vw), 459 (vw), 425 (vw); <sup>1</sup>H NMR (500 MHz, CD<sub>3</sub>OD):  $\delta$  (ppm) = 1.39–1.55 (m, 31H, 2 × CH<sub>2</sub>, 3 × C(CH<sub>3</sub>)<sub>3</sub>), 1.61–1.85 (m,

4H, 2 × CH<sub>2</sub>), 2.97–3.27 (m, 12H, 6 × CH<sub>2</sub>), 3.75 (s, 2H, CH<sub>2</sub>), 3.34–3.41 (m, 1H, NH), 4.18–4.32 (m, 2H, CH<sub>2</sub>), 4.44–4.58 (m, 1H, CHCH<sub>2</sub>), 7.28–7.34 (m, 2H, 2 × CH<sub>ar</sub>), 7.36–7.42 (m, 2H, 2 × CH<sub>ar</sub>), 7.60–7.67 (m, 2H, 2 × CH<sub>ar</sub>), 7.76–7.84 (m, 2H, 2 × CH<sub>ar</sub>), mixture of two rotamers; <sup>13</sup>C NMR was not obtained due to poor signal-to-noise ratio; HRMS  $m/z$  calc for C<sub>42</sub>H<sub>63</sub>N<sub>4</sub>O<sub>10</sub>: 783.4539; found: 783.4533 [M+H]<sup>+</sup>.

#### 4.6.4. 3-(1,4,7,10-Tetraoxa-13-azacyclopentadecan-13-yl)propan-1-amine (**12**)

The preparation and properties of compound **12** have been reported in Ref. [48].

#### 4.6.5. General procedure for the preparation of the diazo transfer reagent TfN<sub>3</sub>

A solution of triflic anhydride (1.85 equiv.) in CH<sub>2</sub>Cl<sub>2</sub> (7.5 mL) was added dropwise to a stirred solution of NaN<sub>3</sub> (9.65 equiv.) in water (4.5 mL) at 0 °C. Afterwards, the reaction mixture was stirred for 2 h at RT. Then, the organic phase was separated and the aqueous phase was extracted with CH<sub>2</sub>Cl<sub>2</sub> (2 × 3.75 mL). Finally, the combined organic layers were washed with brine (4 mL).

4.6.5.1. 13-(3-Azidopropyl)-1,4,7,10-tetraoxa-13-azacyclopentadecane (**13**). The previously prepared TfN<sub>3</sub> solution was added to a solution of primary amine **12** (800 mg, 2.89 mmol), K<sub>2</sub>CO<sub>3</sub> (600 mg, 4.34 mmol) and CuSO<sub>4</sub>·5H<sub>2</sub>O (7.2 mg, 28.9 μmol) in MeOH/H<sub>2</sub>O (2:1, 27 mL). The reaction mixture was stirred overnight at RT. Afterwards, the organic phase was separated and the aqueous phase was extracted with CH<sub>2</sub>Cl<sub>2</sub> (3 × 50 mL). The combined organic layers were dried over MgSO<sub>4</sub> and the solvent was removed under reduced pressure. The product was obtained as brownish liquid: yield 615 mg (70%). IR (KBr):  $\tilde{\nu}$  (cm<sup>-1</sup>) = 3441 (w), 2868 (m), 2096 (s), 1686 (w), 1620 (w), 1561 (vw), 1452 (m), 1356 (m), 1263 (m), 1180 (m), 1125 (s), 1032 (m), 978 (w), 849 (w), 638 (w), 614 (w), 571 (vw), 517 (vw); <sup>1</sup>H NMR (400 MHz, CDCl<sub>3</sub>):  $\delta$  (ppm) = 1.71 (quin, <sup>3</sup>J = 6.9 Hz, 2H, CH<sub>2</sub>), 2.57 (t, <sup>3</sup>J = 6.9 Hz, 2H, CH<sub>2</sub>), 2.72 (t, <sup>3</sup>J = 5.9 Hz, 4H, 2 × CH<sub>2</sub>), 3.34 (quin, <sup>3</sup>J = 6.7 Hz, 2H, CH<sub>2</sub>), 3.59–3.66 (m, 16H, 8 × CH<sub>2</sub>); <sup>13</sup>C NMR (100 MHz, CDCl<sub>3</sub>):  $\delta$  (ppm) = 26.8 (CH<sub>2</sub>), 49.4 (CH<sub>2</sub>), 53.4 (CH<sub>2</sub>), 54.7 (CH<sub>2</sub>), 69.9 (CH<sub>2</sub>), 70.1 (CH<sub>2</sub>), 70.4 (CH<sub>2</sub>), 70.9 (CH<sub>2</sub>); FAB MS:  $m/z$  (%) = 341 (23) [M+K]<sup>+</sup>, 325 (8) [M+Na]<sup>+</sup>, 303 (100) [M+H]<sup>+</sup>, 232 (60) [M–C<sub>2</sub>H<sub>4</sub>N<sub>3</sub>]<sup>+</sup>; HRMS  $m/z$  calc for C<sub>13</sub>H<sub>27</sub>N<sub>4</sub>O<sub>4</sub>: 303.2032; found: 303.2036 [M+H]<sup>+</sup>.

4.6.5.2. 1-(3-(Azidomethyl)phenyl)-N,N,N-trimethylmethanaminium iodide (**17**). The previously prepared TfN<sub>3</sub> solution was added to a solution of primary amine **16** (1.00 g, 2.30 mmol), K<sub>2</sub>CO<sub>3</sub> (954 mg, 6.90 mmol) and CuSO<sub>4</sub>·5H<sub>2</sub>O (5.7 mg, 23.0 μmol) in MeOH/H<sub>2</sub>O (2:1, 27 mL). The reaction mixture was stirred overnight at RT. Afterwards, the organic phase was separated and the aqueous phase was extracted with CH<sub>2</sub>Cl<sub>2</sub> (2 × 50 mL). The combined organic layers were washed with a saturated solution of NaI in H<sub>2</sub>O (20 mL) and the solvent was removed under reduced pressure. The crude product was taken up in a small amount of EtOH and precipitated by the addition of Et<sub>2</sub>O. The precipitate was thoroughly washed with Et<sub>2</sub>O and dried in vacuum. The product was obtained as an off-white solid: yield 309 mg (40%). Mp 127 °C; IR (ATR):  $\tilde{\nu}$  (cm<sup>-1</sup>) = 2999 (w), 2080 (m), 1477 (m), 1445 (w), 1368 (w), 1230 (m), 1161 (w), 1005 (w), 973 (w), 915 (w), 884 (w), 865 (m), 806 (m), 777 (w), 746 (m), 714 (m), 684 (w), 569 (w), 555 (w), 443 (w), 411 (vw); <sup>1</sup>H NMR (300 MHz, CDCl<sub>3</sub>):  $\delta$  (ppm) = 3.43 (s, 9H, 3 × CH<sub>3</sub>), 4.41 (s, 2H, CH<sub>2</sub>), 5.11 (s, 2H, CH<sub>2</sub>), 7.45–7.51 (m, 2H, 2 × CH<sub>ar</sub>), 7.66 (s, 1H, CH<sub>ar</sub>), 7.71 (d, <sup>3</sup>J = 6.5 Hz, 1H, CH<sub>ar</sub>); <sup>13</sup>C NMR (75 MHz, CDCl<sub>3</sub>):  $\delta$  (ppm) = 53.0 (CH<sub>3</sub>), 53.9 (CH<sub>2</sub>), 68.2 (CH<sub>2</sub>), 127.8 (C<sub>ar</sub>), 129.9 (CH<sub>ar</sub>), 130.7 (CH<sub>ar</sub>), 132.7 (CH<sub>ar</sub>), 133.0 (CH<sub>ar</sub>), 136.8 (C<sub>ar</sub>); FAB

MS:  $m/z$  (%) = 205 (100)  $[M]^+$ ; HRMS  $m/z$  calc for  $C_{11}H_{17}N_4$ : 205.1448; found: 205.1450  $[M]^+$ .

#### 4.6.6. *tert*-Butyl 3-(aminomethyl)benzylcarbamate (**14**)

The preparation and properties of compound **9** have been reported in Ref. [66].

#### 4.6.7. 1-(3-(((*tert*-Butoxycarbonyl)amino)methyl)phenyl)-*N,N,N*-trimethylmethanaminium iodide (**15**)

To a solution of primary amine **14** (14.4 g, 61.0 mmol) and  $NaHCO_3$  (51.2 g, 610 mmol) in MeOH (875 mL) was added MeI (38.1 mL, 610 mmol). The resulting mixture was stirred for 2 d at RT. Afterwards, the solution was filtrated and the solvent was removed under reduced pressure. The product was obtained as white solid and was used without further purification. Mp 126 °C; IR (ATR):  $\hat{\nu}$  ( $cm^{-1}$ ) = 3350 (vw), 3006 (w), 2997 (w), 1689 (m), 1517 (w), 1475 (w), 1446 (w), 1393 (w), 1365 (w), 1339 (w), 1248 (w), 1164 (m), 1121 (w), 1045 (w), 1021 (w), 998 (w), 971 (w), 955 (w), 915 (w), 879 (w), 803 (w), 745 (w), 704 (w), 639 (vw), 571 (vw), 442 (w);  $^1H$  NMR (500 MHz,  $CD_3OD$ ):  $\delta$  (ppm) = 1.45 (s, 9H,  $3 \times CH_3$ ), 3.13 (s, 9H,  $3 \times CH_3$ ), 4.29 (s, 2H,  $CH_2$ ), 4.57 (s, 2H,  $CH_2$ ), 7.49 (m, 4H,  $4 \times CH_{ar}$ );  $^{13}C$  NMR (125 MHz,  $CD_3OD$ ):  $\delta$  (ppm) = 28.8 ( $CH_3$ ), 44.7 ( $CH_2$ ), 53.2 ( $CH_3$ ), 53.2 ( $CH_3$ ), 53.3 ( $CH_3$ ), 70.4 ( $CH_2$ ), 80.4 (C), 129.2 ( $C_{ar}$ ), 130.5 ( $CH_{ar}$ ), 130.7 ( $CH_{ar}$ ), 132.7 ( $CH_{ar}$ ), 142.5 ( $C_{ar}$ ), 158.6 (C); FAB MS:  $m/z$  (%) = 279 (100)  $[M]^+$ , 223 (17)  $[M-C_4H_8]^+$ , 178 (2)  $[M-C_5H_9O_2]^+$ , 164 (19)  $[M-C_7H_{17}N]^+$ ; HRMS  $m/z$  calc for  $C_{16}H_{27}N_2O_2$ : 279.2073; found: 279.2069  $[M]^+$ .

#### 4.6.8. 1-(3-(Ammoniomethyl)phenyl)-*N,N,N*-trimethylmethanaminium diiodide (**16**)

To a solution of Boc-protected amine **15** (24.8 g, 61.0 mmol) in  $H_2O$  (525 mL) was added hydroiodic acid (57%, 40.3 mL, 305 mmol). Afterwards, the mixture was stirred overnight at RT. The solution was filtrated and the aqueous phase was washed with  $CH_2Cl_2$  ( $4 \times 200$  mL). The solvent was removed under reduced pressure and the residue was taken up in MeOH (450 mL). Following, the product was precipitated by the addition of EtOAc (900 mL) and washed with EtOAc (300 mL) and MeOH (30 mL). After drying in vacuum, the product was obtained as slightly yellow crystals: yield 18.5 g (70% over two steps). Mp 236 °C; IR (ATR):  $\hat{\nu}$  ( $cm^{-1}$ ) = 3000 (w), 1736 (vw), 1566 (w), 1475 (w), 1441 (w), 1397 (w), 1377 (w), 1365 (w), 1282 (vw), 1234 (vw), 1173 (w), 1124 (vw), 1100 (w), 1070 (w), 1000 (w), 969 (w), 925 (w), 917 (w), 876 (w), 860 (w), 808 (w), 744 (w), 706 (w), 635 (vw), 574 (vw), 483 (vw), 445 (w), 418 (vw);  $^1H$  NMR (500 MHz,  $CD_3OD$ ):  $\delta$  (ppm) = 3.19 (s, 9H,  $3 \times CH_3$ ), 4.26 (s, 2H,  $CH_2$ ), 4.68 (s, 2H,  $CH_2$ ), 7.62–7.65 (m, 1H,  $CH_{ar}$ ), 7.68–7.70 (m, 2H,  $2 \times CH_{ar}$ ), 7.78 (s, 1H,  $CH_{ar}$ );  $^{13}C$  NMR (125 MHz,  $CD_3OD$ ):  $\delta$  (ppm) = 43.9 ( $CH_2$ ), 55.5 ( $CH_3$ ), 55.5 ( $CH_3$ ), 55.6 ( $CH_3$ ), 69.9 ( $CH_2$ ), 130.1 ( $C_{ar}$ ), 131.3 ( $CH_{ar}$ ), 132.6 ( $CH_{ar}$ ), 134.9 ( $CH_{ar}$ ), 134.9 ( $CH_{ar}$ ), 135.7 ( $C_{ar}$ ); FAB MS:  $m/z$  (%) = 179 (100)  $[M]^+$ , 120 (18)  $[M-C_3H_9N]^+$ ; HRMS  $m/z$  calc for  $C_{11}H_{19}N_2$ : 179.1548; found: 179.1550  $[M]^+$ .

#### 4.6.9. (4-Azidobutyl)triphenylphosphonium bromide (**19**)

The preparation and properties of compound **19** have been reported in Ref. [54].

#### 4.6.10. *N*-(2-Azidoethyl)-*N*-methylaniline (**21**)

The preparation and properties of compound **21** have been reported in Ref. [67].

#### 4.6.11. (4-((2-Azidoethyl)methyl)amino)phenyl)bis(4-(dimethylamino)phenyl)methylum chloride (**22**)

Phosphoryl chloride (1.90 mL, 20.8 mmol) was added to a stirred solution of aniline **21** (2.51 g, 14.2 mmol) and 4,4'-

bis(dimethylamino)benzophenone (2.74 g, 10.2 mmol) in toluene (3.8 mL). The reaction mixture was heated overnight at 100 °C. After cooling to RT,  $CH_2Cl_2$  (400 mL) was added and the organic phase was washed with water (20 mL). The solvent was removed under reduced pressure. After purification (chromatography with eluent  $CH_2Cl_2 \rightarrow MeOH$ ) the title compound was obtained as a bronze solid: yield 4.70 g (>99%). Mp 75 °C; IR (KBr):  $\hat{\nu}$  ( $cm^{-1}$ ) = 2853 (w), 2090 (m), 1573 (m), 1476 (w), 1331 (m), 1291 (m), 1160 (m), 938 (m), 909 (m), 822 (w), 757 (w), 717 (w), 663 (w), 619 (w), 557 (w), 506 (w), 418 (w);  $^1H$  NMR (400 MHz,  $CD_3OD$ ):  $\delta$  (ppm) = 3.24–3.27 (m, 15H,  $5 \times CH_3$ ), 3.64 (t,  $^3J = 5.4$  Hz, 2H,  $CH_2$ ), 3.82 (t,  $^3J = 5.4$  Hz, 2H,  $CH_2$ ), 6.93–7.04 (m, 6H,  $6 \times CH_{ar}$ ), 7.26–7.38 (m, 6H,  $6 \times CH_{ar}$ );  $^{13}C$  NMR (100 MHz,  $CD_3OD$ ):  $\delta$  (ppm) = 39.5 ( $CH_3$ ), 40.6 ( $CH_3$ ), 50.3 ( $CH_2$ ), 52.4 ( $CH_2$ ), 113.6 ( $CH_{ar}$ ), 113.7 ( $CH_{ar}$ ), 127.9 ( $C_{ar}$ ), 128.4 ( $C_{ar}$ ), 140.6 ( $CH_{ar}$ ), 141.0 ( $CH_{ar}$ ), 156.4 ( $C_{ar}$ ), 157.5 ( $C_{ar}$ ), 179.8 ( $C_{ar}$ ); FAB MS:  $m/z$  (%) = 427 (100)  $[M]^+$ , 413 (58)  $[M-N]^+$ ; HRMS  $m/z$  calc for  $C_{26}H_{31}N_6$ : 427.2610; found: 427.2608  $[M]^+$ .

#### 4.6.12. General procedure for the synthesis of the peptoids **1** and **2**

Fmoc-protected Rink amide resin (0.64 mmol/g, 50 mg) was swollen in DMF (1 mL) for 1 h. Multiple washing steps using DMF were performed between each step as described below. Fmoc deprotection was completed by adding piperidine (20% in DMF, 1 mL,  $3 \times 5$  min). Following the respective peptoid monomer was coupled to the resin. To achieve this, the monomer **10** or **11** (96.0  $\mu$ mol, 3 equiv.), diisopropylcarbodiimide (15.0  $\mu$ L, 96.0  $\mu$ mol) and 1-hydroxybenzotriazole hydrate (14.7 mg, 96.0  $\mu$ mol) were dissolved in DMF *biograde* (1 mL) and added to the resin. The reaction vessel was subjected to microwave irradiation to keep the constant temperature at 60 °C (max. 20 W) for 30 min while being stirred. The reaction solution was filtered and the resin was treated a second time with freshly prepared reaction solution under the same conditions as described above (double coupling). Afterwards, the resin was thoroughly washed with DMF ( $5 \times 3$  mL). This procedure of Fmoc deprotection and monomer coupling was repeated six times in total, so that a resin bound hexamer was obtained. Then another Fmoc deprotection step was carried out under the previously described conditions. Subsequently, a solution of rhodamine B (46.0 mg, 96.0  $\mu$ mol), diisopropylcarbodiimide (15.0  $\mu$ L, 96.0  $\mu$ mol) and 1-hydroxybenzotriazole hydrate (14.7 mg, 96.0  $\mu$ mol) in DMF *biograde* (1 mL) was added to the washed resin. A double coupling was performed under the same conditions (microwave irradiation: 60 °C for 30 min) as described for the coupling of the monomer. Afterwards, the resin was thoroughly washed with DMF until the washing solution remained colorless. For the final cleavage the resin was incubated overnight with TFA (95% in  $CH_2Cl_2$ , 2 mL) at RT. Following, the resin was washed with MeOH until the washing solution remained colorless. The crude product was lyophilized and purified by HPLC.

4.6.12.1. *Peptoid 1*. After purification the title compound was obtained as red solid: yield 15.9 mg (17% over 15 steps). Analytical HPLC (5–95% acetonitrile + 0.1% TFA in 30 min,  $t_{ret} = 9.9$  min) purity: 98%; MALDI-TOF MS:  $m/z = 1458$   $[M+H]^+$ .

4.6.12.2. *Peptoid 2*. After purification the title compound was obtained as red solid: yield 1.77 mg (1.4% over 15 steps). Analytical HPLC (5–95% acetonitrile + 0.1% TFA in 30 min,  $t_{ret} = 8.9$  min) purity: 98%; MALDI-TOF MS:  $m/z = 1896$   $[M+H]^+$ .

#### 4.6.13. *Peptoid 3*

Fmoc-protected Rink amide resin (0.64 mmol/g, 100 mg) was swollen in DMF (2 mL) for 1 h. Multiple washing steps using DMF ( $5 \times 3$  mL) were performed between each step as described below.

Fmoc deprotection was completed by adding piperidine (20% in DMF, 2 mL, 3 × 5 min). Afterwards a solution of bromoacetic acid (89.0 mg, 640 μmol) and diisopropylcarbodiimide (99.7 μL, 640 μmol) in 640 μL DMF *biograde* was added to the resin. The reaction mixture was shaken for 30 min at RT. Next, a solution of propargylamine (34.0 μL, 531 μmol) in 530 μL DMF *biograde* was added and the mixture was shaken for 1 h at RT. This procedure of acylation with bromoacetic acid and amination with propargylamine was repeated six times in total, so that a resin bound hexamer was obtained. The side chains were functionalized by adding a solution of azide **13** (406 mg, 1.36 mmol), 2,6-lutidine (358 μL, 3.07 mmol), and tetrakis(acetonitrile)copper(I) hexafluorophosphate (143 mg, 384 μmol) in THF (1.9 mL) to the washed resin. After shaking for 2.5 d at RT, the resin was thoroughly washed with DMF. Subsequently, a solution of rhodamine B (92.0 mg, 192 μmol), diisopropylcarbodiimide (29.9 μL, 192 μmol) and 1-hydroxybenzotriazole hydrate (29.4 mg, 192 μmol) in DMF *biograde* (2 mL) was added to the washed resin. The reaction vessel was subjected to microwave irradiation to keep the constant temperature at 60 °C (max. 20 W) for 30 min while being stirred. The reaction solution was filtered and the resin was treated a second time with freshly prepared reaction solution under the same conditions as described above (double coupling). Afterwards, the resin was thoroughly washed with DMF until the washing solution remained colorless. For the final cleavage the resin was incubated for 3 × 30 min with TFA (95% in CH<sub>2</sub>Cl<sub>2</sub>, 3 mL) at RT. Following, the resin was washed with MeOH until the washing solution remained colorless. The crude product was lyophilized and purified by HPLC. After purification the title compound was obtained as red solid: yield 3.49 mg (1.5% over 16 steps). Analytical HPLC (5–95% acetonitrile + 0.1% TFA in 30 min,  $t_{\text{ret}} = 14.2$  min) purity: 89%; MALDI-TOF MS:  $m/z = 2826$  [M]<sup>+</sup>.

#### 4.6.14. 2-(((9H-Fluoren-9-yl)methoxy)carbonyl)(6-((tert-butoxycarbonyl)amino)hexyl)amino)acetic acid

The preparation and properties of the title compound have been reported in Ref. [46].

#### 4.6.15. General procedure for the synthesis of the peptoids **4** and **5**

Fmoc-protected Rink amide resin (0.64 mmol/g, 100 mg) was swollen in DMF (2 mL) for 1 h. Multiple washing steps using DMF (5 × 3 mL) were performed between each step as described below. Fmoc deprotection was completed by adding piperidine (20% in DMF, 2 mL, 3 × 5 min). The first monomer was introduced by the submonomer method. A solution of bromoacetic acid (89.0 mg, 640 μmol) and diisopropylcarbodiimide (99.5 μL, 640 μmol) in 640 μL DMF *biograde* was added to the resin. The reaction mixture was shaken for 30 min at RT. Next, a solution of propargylamine (34.0 μL, 531 μmol) in 530 μL DMF *biograde* was added and the mixture was shaken for 1 h at RT. Following, the peptoid monomer 2-(((9H-fluoren-9-yl)methoxy)carbonyl)(6-((tert-butoxycarbonyl)amino)hexyl)amino)acetic acid was introduced. To achieve this, the monomer (95.5 mg, 192 μmol), diisopropylcarbodiimide (29.9 μL, 192 μmol) and 1-hydroxybenzotriazole hydrate (29.4 mg, 192 μmol) were dissolved in DMF *biograde* (2 mL) and added to the resin. The reaction vessel was subjected to microwave irradiation to keep the constant temperature at 60 °C (max. 20 W) for 30 min while being stirred. The reaction solution was filtered and the resin was treated a second time with freshly prepared reaction solution under the same conditions as described above (double coupling). Next, the Fmoc protecting group was removed as described above. The same monomer was introduced once more under equal conditions (double coupling with microwave irradiation). The sequence of submonomer coupling with propargylamine and two monomer coupling steps with 2-(((9H-fluoren-9-yl)

methoxy)carbonyl)(6-((tert-butoxycarbonyl)amino)hexyl)amino)acetic acid was repeated once more to obtain a resin bound hexamer. Then another Fmoc deprotection step was carried out under the previously described conditions. Subsequently, a solution of rhodamine B (92.0 mg, 192 μmol), diisopropylcarbodiimide (29.9 μL, 192 μmol) and 1-hydroxybenzotriazole hydrate (29.4 mg, 192 μmol) in DMF *biograde* (2 mL) was added to the washed resin. A double coupling was performed under the same conditions (microwave irradiation: 60 °C for 30 min) as described for the coupling of the monomer. Afterwards, the resin was thoroughly washed with DMF until the washing solution remained colorless. Finally, the respective azide was introduced. A solution of azide **19** or **22** (384 μmol, 6 equiv.), 2,6-lutidine (59.7 μL, 512 μmol), and tetrakis(acetonitrile)copper(I) hexafluorophosphate (47.7 mg, 128 μmol) in THF was added to the resin and shaken at RT. Afterwards, the resin was thoroughly washed with DMF. For the final cleavage the resin was incubated with TFA (95% in CH<sub>2</sub>Cl<sub>2</sub>) at RT. Following, the resin was washed with MeOH until the washing solution remained colorless. The crude product was lyophilized and purified by HPLC.

4.6.15.1. *Peptoid 4*. Azide **19** was dissolved in 1.9 mL THF and shaken for 1.5 d at RT. The cleavage was performed with 3 mL TFA (95% in CH<sub>2</sub>Cl<sub>2</sub>, 3 × 30 min). After purification the title compound was obtained as red solid: yield 2.36 mg (1.3% over 16 steps). Analytical HPLC (5–95% acetonitrile + 0.1% TFA in 30 min,  $t_{\text{ret}} = 12.3$  min) purity: 85%; MALDI-TOF MS:  $m/z = 1976$  [M+H]<sup>+</sup>.

4.6.15.2. *Peptoid 5*. Azide **22** was dissolved in 3.8 mL THF and shaken for 1.5 d at RT. Afterwards, the reaction solution was filtered and the resin was treated a second time with freshly prepared reaction solution. The mixture was shaken again for 2 d at RT. The cleavage was performed with 3 mL TFA (95% in CH<sub>2</sub>Cl<sub>2</sub>, 30 min). After purification the title compound was obtained as violet solid: yield 0.69 mg (0.4% over 16 steps). Analytical HPLC (5–95% acetonitrile + 0.1% TFA in 30 min,  $t_{\text{ret}} = 13.6$  min) purity: 98%; MALDI-TOF MS:  $m/z = 2111$  [M+H]<sup>+</sup>.

#### 4.7. Crystal structure determination of **16**

The single-crystal X-ray diffraction study was carried out on a Bruker-Nonius Kappa-CCD diffractometer at 123(2) K using MoK $\alpha$  radiation ( $\lambda = 0.71073$  Å). Direct Methods (SHELXS-97) [68] were used for structure solution and refinement was carried out using SHELXL-97 [68] (full-matrix least-squares on  $F^2$ ). Non hydrogen atoms were refined anisotropically, hydrogen atoms were localized by difference electron density determination and refined using a riding model (H(N) free). A semi-empirical absorption correction was applied.

**16**: colorless crystals, C<sub>11</sub>H<sub>20</sub>N<sub>2</sub><sup>2+</sup> – 2 I<sup>−</sup>,  $M = 434.09$ , crystal size 0.30 × 0.12 × 0.06 mm, monoclinic, space group P2<sub>1</sub>/n (No. 14),  $a = 5.3325(4)$  Å,  $b = 17.0104(17)$  Å,  $c = 16.4987(11)$  Å,  $\beta = 96.915(7)^\circ$ ,  $V = 1485.7(2)$  Å<sup>3</sup>,  $Z = 4$ ,  $\rho(\text{calc}) = 1.941$  Mg m<sup>−3</sup>,  $F(000) = 824$ ,  $\mu = 4.210$  mm<sup>−1</sup>, 11882 reflections ( $2\theta_{\text{max}} = 55^\circ$ ), 3338 unique [ $R_{\text{int}} = 0.038$ ], 145 parameters, 9 restraints,  $R1$  (for  $2957 I > 2\sigma(I)$ ) = 0.024,  $wR2$  (all data) = 0.055,  $S = 1.04$ , largest diff. peak and hole 0.822 and −0.745 e Å<sup>−3</sup>.

Crystallographic data (excluding structure factors) for the structure reported in this work have been deposited with the Cambridge Crystallographic Data Centre as supplementary publication no. CCDC 969830 (**16**). Copies of the data can be obtained free of charge on application to The Director, CCDC, 12 Union Road, Cambridge CB2 1EZ, UK (Fax: int.code+(1223)336-033; e-mail: deposit@ccdc.cam.ac.uk).

## Acknowledgments

This work was supported by a Feasibility Studies of Young Scientists (FYS) of the KIT (fellowship to D.K.K.), the Fonds der Chemischen Industrie (fellowship to D.K.K.), the Karlsruhe School of Optics & Photonics (fellowship to D.K.K. and A.H.) the Carl-Zeiss foundation (fellowship to A.H.) and the Helmholtz program Bio-interface (F.R., U.S., and S.B.) The authors gratefully acknowledge the help of Karolin Niessner for her assistance on preparative HPLC purification of the compounds.

## Appendix A. Supplementary data

Supplementary data related to this article can be found at <http://dx.doi.org/10.1016/j.ejmech.2014.03.078>.

## References

- [1] M. Green, P.M. Loewenstein, Autonomous functional domains of chemically synthesized human immunodeficiency virus tat trans-activator protein, *Cell* 55 (1988) 1179–1188.
- [2] A.D. Frankel, C.O. Pabo, Cellular uptake of the tat protein from human immunodeficiency virus, *Cell* 55 (1988) 1189–1193.
- [3] a) M.C. Morris, S. Deshayes, F. Heitz, G. Divita, Cell-penetrating peptides: from molecular mechanisms to therapeutics, *Biologie Cellulaire* 100 (2008) 201–217; b) F. Heitz, M.C. Morris, G. Divita, Twenty years of cell-penetrating peptides: from molecular mechanisms to therapeutics, *British Journal of Pharmacology* 157 (2009) 195–206.
- [4] F. Eudes, A. Chugh, Cell-penetrating peptides: from mammalian to plant cells, *Plant Signaling & Behaviour* 3 (2008) 549–550.
- [5] K.M. Stewart, K.L. Horton, S.O. Kelley, Cell-penetrating peptides as delivery vehicles for biology and medicine, *Organic & Biomolecular Chemistry* 6 (2008) 2242–2255.
- [6] E. Vivès, J. Schmidt, A. Pèlerin, Cell-penetrating and cell-targeting peptides in drug delivery, *Biochimica et Biophysica Acta* 1786 (2008) 126–138.
- [7] S. Deshayes, M.C. Morris, G. Divita, F. Heitz, Cell-penetrating peptides: tools for intracellular delivery of therapeutics, *Cellular and Molecular Life Sciences* 62 (2005) 1839–1849.
- [8] a) D.C. Anderson, E. Nichols, R. Manger, D. Woodle, M. Barry, A.R. Fritzberg, Tumor cell retention of antibody Fab fragment is enhanced by an attached HIV TAT protein-derived peptide 194 (1993) 876–884; b) S. Fawell, J. Seery, Y. Daikh, C. Moore, L.L. Chen, B. Pepinsky, J. Barsoum, Tat-mediated delivery of heterologous proteins into cells, *Proceedings of the National Academy of Sciences* 91 (1994) 664–668; c) H. Nagahara, A.M. Vocero-Akbani, E.L. Snyder, A. Ho, D.G. Latham, N.A. Lissy, M. Becker-Hapak, S.A. Ezhevsky, S.F. Dowdy, Transduction of full-length TAT fusion proteins into mammalian cells: TAT-p27<sup>Kip1</sup> induces cell migration, *Natural Medicines* 4 (1998) 1449–1452.
- [9] a) D. Derossi, S. Calvet, A. Trembleau, A. Brunissen, G. Chassaing, A. Prochiantz, Cell internalization of the third helix of the antennapedia homeodomain is receptor-independent, *Journal of Biological Chemistry* 271 (1996) 18188–18193; b) A. Prochiantz, Getting hydrophilic compounds into cells: lessons from homeopeptides, *Current Opinion In Neurobiology* 6 (1996) 629–634; c) D. Derossi, G. Chassaing, A. Prochiantz, Trojan peptides: the penetratin system for intracellular delivery, *Trends in Cell Biology* 8 (1998) 84–87; d) S.R. Schwarze, S.F. Dowdy, In vivo protein transduction: intracellular delivery of biologically active proteins, compounds and DNA, *Trends in Pharmacological Sciences* 21 (2000) 45–48.
- [10] a) M. Pooga, M. Hällbrink, M. Zorko, Ü. Langel, Cell penetration by transportan, *FASEB Journal* 12 (1998) 67–77; b) M. Pooga, M. Lindgren, M. Hällbrink, E. Bräkenhielm, Ü. Langel, Galanin-based peptides, galparan and transportan, with receptor-dependent and independent activities, *Annals of the New York Academy of Sciences* 863 (1998) 450–453.
- [11] a) N. Emi, S. Kidoaki, K. Yoshikawa, H. Saito, Gene transfer mediated by polyarginine requires a formation of big carrier-complex of DNA aggregate, *Biochemical and Biophysical Research* 231 (1997) 421–424; b) K. Takayama, A. Tadokoro, S. Pujals, I. Nakase, E. Giral, S. Futaki, Novel system to achieve one-pot modification of cargo molecules with oligoarginine vectors for intracellular delivery, *Bioconjugate Chemistry* 20 (2009) 249–257; c) N.A. Alhakamy, C.J. Berkland, Polyarginine molecular weight determines transfection efficiency of calcium condensed complexes, *Molecular Pharmaceutics* 10 (2013) 1940–1948.
- [12] a) M. Rueping, Y. Mahajan, M. Sauer, D. Seebach, Cellular uptake studies with  $\beta$ -peptides, *ChemBioChem* 3 (2002) 257–259; b) T.B. Potocky, A.K. Menon, S.H. Gellman, Cytoplasmic and nuclear delivery of a TAT-derived peptide and a  $\beta$ -peptide after endocytic uptake into HeLa cells, *Journal of Biological Chemistry* 278 (2003) 50188–50194.
- [13] P.A. Wender, J.B. Rothbard, T.C. Jessop, E.L. Kreider, B.L. Wylie, Oligocarbamate molecular transporters: design, synthesis, and biological evaluation of a new class of transporters for drug delivery, *Journal of the American Chemical Society* 124 (2002) 13382–13383.
- [14] a) S.M. Miller, R.J. Simon, S. Ng, R.N. Zuckermann, J.M. Kerr, W.H. Moos, Proteolytic studies of homologous peptide and N-substituted glycine peptoid oligomers, *Bioorganic & Medicinal Chemistry Letters* 4 (1994) 2657–2662; b) J.V. Schreiber, J. Frackenhohl, F. Moser, T. Fleischmann, H.-P.E. Kohler, D. Seebach, On the biodegradation of  $\beta$ -peptides, *ChemBioChem* 3 (2002) 424–432; c) J. Farrera-Sinfreu, E. Giral, M. Royo, F. Albericio, Cell-penetrating proline-rich peptidomimetics, *Methods in Molecular Biology* 386 (2007) 241–267; d) J.-K. Bang, Y.H. Nan, E.K. Lee, S.Y. Shin, A novel Trp-rich model antimicrobial peptoid with increased protease stability, *Bulletin of the Korean Chemical Society* 31 (2010) 2509–2513.
- [15] E. Koren, V.P. Torchilin, Cell-penetrating peptides: breaking through to the other side, *Trends in Molecular Medicine* 18 (2012) 385–393.
- [16] I. Peretto, R.M. Sanchez-Martin, X.-h. Wang, J. Ellard, S. Mittoo, M. Bradley, Cell penetrable peptoid carrier vehicles: synthesis and evaluation, *Chemical Communications* (2003) 2312–2313.
- [17] M.E. Herbig, U. Fromm, J. Leuenberger, U. Krauss, A.G. Beck-Sickinger, H.P. Merkle, Bilayer interaction and localization of cell penetrating peptides with model membranes: a comparative study of a human calcitonin (hCT)-derived peptide with pVEC and pAntp(43–58), *Biochimica et Biophysica Acta* 1712 (2005) 197–211.
- [18] a) T. Suzuki, S. Futaki, M. Niwa, S. Tanaka, K. Ueda, Y. Sugiura, Possible existence of common internalization mechanisms among arginine-rich peptides, *Journal of Biological Chemistry* 277 (2002) 2437–2443; b) W.P.R. Verdurmen, P.H. Bovee-Geurts, P. Wadhvani, A.S. Ulrich, M. Hällbrink, T.H. van Kuppevelt, R. Brock, Preferential uptake of L-versus D-amino acid cell-penetrating peptides in a cell type-dependent manner, *Chemistry & Biology* 18 (2011) 1000–1010.
- [19] F. Madani, S. Lindberg, Ü. Langel, S. Futaki, A. Gräslund, Mechanisms of cellular uptake of cell-penetrating peptides, *Journal of Biophysics* 2011 (2011) 1–10.
- [20] S. Trabulo, A.L. Cardoso, M. Mano, M.C.P. de Lima, Cell-penetrating peptide-mechanisms of cellular uptake and generation of delivery systems, *Pharmaceuticals* 3 (2010) 961–993.
- [21] N.P. Chongsirawatana, J.A. Patch, A.M. Czyzewski, M.T. Dohm, A. Ivankin, D. Gidalevitz, R.N. Zuckermann, A.E. Barron, Peptoids that mimic the structure, function, and mechanism of helical antimicrobial peptides, *Proceedings of the National Academy of Sciences of the United States of America* 105 (2008) 2794–2799.
- [22] a) T.S. Burkoth, E. Beausoleil, S. Kaur, D. Tang, F.E. Cohen, R.N. Zuckermann, Towards the synthesis of artificial proteins: the discovery of an amphiphilic helical peptoid assembly, *Chemistry & Biology* 9 (2002) 647–654; b) H.K. Murnen, A.M. Rosales, J.N. Jaworski, R.A. Segalman, R.N. Zuckermann, Hierarchical self-assembly of a biomimetic diblock copolypeptoid into homochiral superhelices, *Journal of the American Chemical Society* 132 (2010) 16112–16119; c) J.R. Stringer, J.A. Crapster, I.A. Guzei, H.E. Blackwell, Extraordinarily robust polyproline type I peptoid helices generated via the incorporation of  $\alpha$ -chiral aromatic N-1-naphthylethyl side chains, *Journal of the American Chemical Society* 133 (2011) 15559–15567.
- [23] a) K.T. Nam, S.A. Shelby, P.H. Choi, A.B. Marciel, R. Chen, L. Tan, T.K. Chu, R.A. Mesch, B.-C. Lee, M.D. Connolly, C. Kisielowski, R.N. Zuckermann, Free-floating ultrathin two-dimensional crystals from sequence-specific peptoid polymers, *Nature Materials* 9 (2010) 454–460; b) B. Sanii, R. Kudirka, A. Cho, N. Venkateswaran, G.K. Oliver, A.M. Olson, H. Tran, R.M. Harada, L. Tan, R.N. Zuckermann, Shaken, not stirred: collapsing a peptoid monolayer to produce free-floating, stable nanosheets, *Journal of the American Chemical Society* 133 (2011) 20808–20815; c) J.A. Crapster, J.R. Stringer, I.A. Guzei, H.E. Blackwell, Design and conformational analysis of peptoids containing N-hydroxy amides reveals a unique sheet-like secondary structure, *Biopolymers (Peptide Sciences)* 96 (2011) 604–616.
- [24] K. Huang, C.W. Wu, T.J. Sanborn, J.A. Patch, K. Kirshenbaum, R.N. Zuckermann, A.E. Barron, I. Radhakrishnan, A threaded loop conformation adopted by a family of peptoid nonamers, *Journal of the American Chemical Society* 128 (2006) 1733–1738.
- [25] J.A. Crapster, I.A. Guzei, H.E. Blackwell, A peptoid ribbon secondary structure, *Angewandte Chemie* 125 (2013) 5183–5188. *Angew. Chem. Int. Ed.* 52(2013) 5079–5084.
- [26] J.R. Stringer, J.A. Crapster, I.A. Guzei, H.E. Blackwell, Construction of peptoids with all trans-amide backbones and peptoid reverse turns via the tactical incorporation of N-aryl side chains capable of hydrogen bonding, *Journal of Organic Chemistry* 75 (2010) 6068–6078.
- [27] a) K. Eggenberger, E. Birtalan, T. Schröder, S. Bräse, P. Nick, Passage of Trojan peptoids into plant cells, *ChemBioChem* 10 (2009) 2504–2512; b) E. Birtalan, B. Rudat, D.K. Kölmel, D. Fritz, S.B.L. Vollrath, U. Schepers, S. Bräse, Investigating rhodamine B-labeled peptoids: scopes and limitations of its applications, *Biopolymers (Peptide Sciences)* 96 (2011) 694–701.
- [28] E.A. Goun, T.H. Pillow, L.R. Jones, J.B. Rothbard, P.A. Wender, Molecular transporters and their application to drug delivery and real-time imaging, *ChemBioChem* 7 (2006) 1497–1515.

- [29] Y. Utku, E. Dehan, O. Ouerfelli, F. Piano, R.N. Zuckermann, M. Pagano, K. Kirshenbaum, A peptidomimetic siRNA transfection reagent for highly effective gene silencing, *Molecular Biosystems* 2 (2006) 312–317.
- [30] J. Lee, D.G. Udugamasooriya, H.-S. Lim, T. Kodadek, Potent and selective photo-inactivation of proteins with peptoid-ruthenium conjugates, *Nature Chemical Biology* 6 (2010) 258–260.
- [31] a) B. Rudat, E. Birtalan, S.B.L. Vollrath, D. Fritz, D.K. Kölmel, M. Nieger, U. Schepers, K. Müllen, H.-J. Eisler, U. Lemmer, S. Bräse, Photophysical properties of fluorescently-labeled peptoids, *European Journal of Medicinal Chemistry* 46 (2011) 4457–4465;  
b) D.K. Kölmel, B. Rudat, D.M. Braun, C. Bednarek, U. Schepers, S. Bräse, Rhodamine F: a novel class of fluorosonyl dyes for bioconjugation, *Organic & Biomolecular Chemistry* 11 (2013) 3954–3962.
- [32] D.K. Kölmel, B. Rudat, U. Schepers, S. Bräse, Peptoid-based rare-earth (group 3 and lanthanide) transporters, *European Journal of Organic Chemistry* (2013) 2761–2765.
- [33] a) M.A. Fara, J.J. Díaz-Mochón, M. Bradley, Microwave-assisted coupling with DIC/HOBt for the synthesis of difficult peptoids and fluorescently labeled peptides – a gentle heat goes a long way, *Tetrahedron Letters* 47 (2006) 1011–1014;  
b) A. Unciti-Broceta, F. Diezmann, C.Y. Ou-Yang, M.A. Fara, M. Bradley, Synthesis, penetrability and intracellular targeting of fluorescein-tagged peptoids and peptide-peptoid hybrids, *Bioorganic & Medicinal Chemistry* 17 (2009) 956–966.
- [34] R.N. Zuckermann, J.M. Kerr, S.B.H. Kent, W.H. Moos, Efficient method for the preparation of peptoids [oligo(*N*-substituted glycines)] by submonomer solid-phase synthesis, *Journal of the American Chemical Society* 114 (1992) 10647–10649.
- [35] G.M. Gigliozzi, R. Goldsmith, S.C. Ng, S.C. Banville, R.N. Zuckermann, Synthesis of *N*-substituted glycine peptoid libraries, *Methods in Enzymology* 167 (1996) 437–447.
- [36] a) J.A.W. Kruijtzter, R.M. Liskamp, Synthesis in solution of peptoids using Fmoc-protected *N*-substituted Glycines, *Tetrahedron Letters* 36 (1995) 6969–6972;  
b) C. Caumes, T. Hjelmggaard, R. Remuson, S. Faure, C. Taillefumier, Highly convenient Gram-scale solution-phase peptoid synthesis and orthogonal side-chain post-modification, *Synthesis* (2011) 257–264.
- [37] D.K. Kölmel, D. Fűrmiss, S. Susanto, A. Lauer, C. Grabher, S. Bräse, U. Schepers, Cell Penetrating Peptoids (CPPos): synthesis of a small combinatorial library by using IRORI MiniKans, *Pharmaceuticals* 5 (2012) 1265–1281.
- [38] J. Sun, R.N. Zuckermann, Peptoid polymers: a highly designable bioinspired material, *ACS Nano* 7 (2013) 4715–4732.
- [39] a) R. Kapoor, P.E. Eimerman, J.W. Hardy, J.D. Cirillo, C.H. Contag, A.E. Barron, Efficacy of antimicrobial peptoids against *Mycobacterium tuberculosis*, *Antimicrobial Agents and Chemotherapy* 55 (2011) 3058–3062;  
b) A.R. Statz, J.P. Park, N.P. Chonsiriwatana, A.E. Barron, P.B. Messersmith, Surface-immobilized antimicrobial peptoids, *Biofouling* 24 (2008) 439–448.
- [40] A.R. Statz, R.J. Meagher, A.E. Barron, P.B. Messersmith, New peptidomimetic polymers for antifouling surfaces, *Journal of the American Chemical Society* 127 (2005) 7972–7973.
- [41] J. Sun, G.M. Stone, N.P. Balsara, R.N. Zuckermann, Structure–conductivity relationship for peptoid-based PEO-mimetic polymer electrolytes, *Macromolecules* 45 (2012) 5151–5156.
- [42] S.B.L. Vollrath, C. Hu, S. Bräse, K. Kirshenbaum, Peptoid nanotubes: an oligomer macrocycle that reversibly sequesters water via single-crystal-to-single-crystal transformations, *Chemical Communications* 49 (2013) 2317–2319.
- [43] a) B.-C. Lee, T.K. Chu, K.A. Dill, R.N. Zuckermann, Biomimetic nanostructures: creating a high-affinity zinc-binding site in a folded nonbiological polymer, *Journal of the American Chemical Society* 130 (2008) 8847–8855;  
b) G. Maayan, M.D. Ward, K. Kirshenbaum, Metallopeptoids, *Chemical Communications* (2009) 56–58.
- [44] [a] D.B. Robinson, G.M. Buffleben, M.E. Langham, R.N. Zuckermann, Stabilization of nanoparticles under biological assembly conditions using peptoids, *Biopolymers (Peptide Sciences)* 96 (2011) 669–678.
- [45] J. Seo, G. Ren, H. Liu, Z. Miao, M. Park, Y. Wang, T.M. Miller, A.E. Barron, Z. Cheng, In vivo biodistribution and small animal PET of <sup>64</sup>Cu-labeled antimicrobial peptoids, *Bioconjugate Chemistry* 23 (2012) 1069–1079.
- [46] T. Schröder, K. Schmitz, N. Niemeier, T.S. Balaban, H.F. Krug, U. Schepers, S. Bräse, Solid-phase synthesis, bioconjugation, and toxicology of novel cationic oligopeptoids for cellular drug delivery, *Bioconjugate Chemistry* 18 (2007) 342–354.
- [47] A.J. Geall, I.S. Blagbrough, Homologation of polyamines in the rapid synthesis of lipospermine conjugates and related lipoplexes, *Tetrahedron* 56 (2000) 2449–2460.
- [48] Y. Guminski, M. Grousseau, S. Cugnasse, V. Brel, J.-P. Annereau, S. Vispé, N. Guilbaud, J.-M. Barret, C. Bailly, T. Imbert, Synthesis of conjugated spermine derivatives with 7-nitrobenzoxadiazole (NBD), rhodamine and bodipy as new fluorescent probes for the polyamine transport system, *Bioorganic & Medicinal Chemistry Letters* 19 (2009) 2474–2477.
- [49] P.D. Beer, A.R. Graydon, New anion receptors based on cobalticinium-aza crown ether derivatives, *Journal of Organometallic Chemistry* 466 (1994) 241–247.
- [50] [a] A. Masuyama, Y. Nakatsuji, I. Ikeda, M. Okahara, Complexing ability of *N*-oligoethylene glycol monoaza crown ethers with sodium and potassium cations, *Tetrahedron Letters* 22 (1981) 4665–4668;  
[b] H. Tsukube, T. Inoue, K. Hori, Li<sup>+</sup> ion-selective binding and transport properties of 12-membered ring lariat ethers: experimental and computational studies on crown ring-sidearm cooperativity, *Journal of Organic Chemistry* 59 (1994) 8047–8052;  
[c] K. Hori, H. Tsukube, Strategy for designing new Li<sup>+</sup> ion specific receptors. A combination of theoretical calculations and experimental techniques, *Journal of Inclusion Phenomena and Macrocyclic Chemistry* 32 (1998) 311–329;  
[d] V. Novakova, L. Lochman, I. Zájíková, K. Kopecky, M. Miletin, K. Lang, K. Kirakci, P. Zimcik, Azaphthalocyanines: red fluorescent probes for cations, *Chemistry – A European Journal* 19 (2013) 5025–5028.
- [51] [a] V.V. Rostovtsev, L.G. Green, V.V. Fokin, K.B. Sharpless, A stepwise Huisgen cycloaddition process: copper(I)-catalyzed regioselective “ligation” of azides and terminal alkynes, *Angewandte Chemie* 114 (2002) 2708–2711. *Angew. Chem. Int. Ed.* 41(2002) 2596–2599;  
[b] C.W. Tornøe, C. Christensen, M. Meldal, Peptidotriazoles on solid phase: [1,2,3]-triazoles by regioselective copper(I)-catalyzed 1,3-dipolar cycloadditions of terminal alkynes to azides, *Journal of Organic Chemistry* 67 (2002) 3057–3064.
- [52] [a] H. Jang, A. Fafarman, J.M. Holub, K. Kirshenbaum, Click to fit: versatile polyvalent display on a peptidomimetic scaffold, *Organic Letters* 7 (2005) 1951–1954;  
[b] J.M. Holub, H. Jang, K. Kirshenbaum, Clickity-click: highly functionalized peptoid oligomers generated by sequential conjugation reactions on solid-phase support, *Organic & Biomolecular Chemistry* 4 (2006) 1497–1502;  
[c] J.M. Holub, M.J. Garabedian, K. Kirshenbaum, Peptoids on steroids: precise multivalent estradiol-peptidomimetic conjugates generated via Azide-Alkyne [3+2] cycloaddition reactions, *QSAR & Combinatorial Science* 26 (2007) 1175–1180;  
[d] J.M. Holub, H. Jang, K. Kirshenbaum, Fit to be tied: conformation-directed macrocyclization of peptoid foldamers, *Organic Letters* 9 (2007) 3275–3278;  
[e] A.S. Norgren, C. Budke, Z. Majer, C. Heggemann, T. Koop, N. Sewald, On-resin click-glycoconjugation of peptoids, *Synthesis* (2009) 488–494;  
[f] Y. Gao, T. Kodadek, Synthesis and screening of stereochemically diverse combinatorial libraries of peptide tertiary amides, *Chemistry & Biology* 20 (2013) 360–369;  
[g] D. Fűrmiss, T. Mack, F. Hahn, S.B.L. Vollrath, K. Koroniak, U. Schepers, S. Bräse, Peptoids and polyamines going sweet: modular synthesis of glycosylated peptoids and polyamines using click chemistry, *Beilstein Journal of Organic Chemistry* 9 (2013) 56–63;  
[h] S.B.L. Vollrath, D. Fűrmiss, U. Schepers, S. Bräse, Amphiphilic peptoid transporters – synthesis and evaluation, *Organic & Biomolecular Chemistry* 11 (2013) 8197–8201;  
[i] A. Höpner, D. Volz, T. Hagendorf, D. Fűrmiss, L. Greb, F. Rönicke, M. Nieger, U. Schepers, S. Bräse, Switchable fluorescence by click reaction of novel azidocarbazole dye, *RSC Advances* 4 (2014) 11528–11534.
- [53] P.T. Nyffeler, C.-H. Liang, K.M. Koeller, C.-H. Wong, The chemistry of amine-azide interconversion: catalytic diazotransfer and regioselective azide reduction, *Journal of the American Chemical Society* 124 (2002) 10773–10778.
- [54] [a] M.F. Ross, G.F. Kelso, F.H. Blaikie, A.M. James, H.M. Cochemé, A. Filipovska, T. Da Ros, T.R. Hurd, R.A.J. Smith, M.P. Murphy, Lipophilic triphenylphosphonium cations as tools in mitochondrial bioenergetics and free radical biology, *Biochemistry (Moscow)* 70 (2005) 222–230;  
[b] Y.-S. Kim, C.-T. Yang, J. Wang, L. Wang, Z.-B. Li, X. Chen, S. Liu, Effects of targeting moiety, linker, bifunctional chelator, and molecular charge on biological properties of <sup>64</sup>Cu-labeled triphenylphosphonium cations, *Journal of Medicinal Chemistry* 51 (2008) 2971–2984;  
[c] J. Jiang, D.A. Stoyanovsky, N.A. Belikova, Y.Y. Tyurina, Q. Zhao, M.A. Tungekar, V. Kapralova, Z. Huang, A.H. Mintz, J.S. Greenberger, V.E. Kagan, A mitochondria-targeted triphenylphosphonium-conjugated nitroxide functions as a radioprotector/mitigator, *Radiation Research* 172 (2009) 709–717.
- [55] X. Chen, G.N. Khairallah, R.A.J. O’Hair, S.J. Williams, Fixed-charge labels for simplified reaction analysis: 5-hydroxy-1,2,3-triazoles as byproducts of a copper(I)-catalyzed click reaction, *Tetrahedron Letters* 52 (2011) 2750–2753.
- [56] I.K. Kandela, W. Lee, G.L. Indig, Effect of the lipophilic/hydrophilic character of cationic triarylmethane dyes on their selective phototoxicity toward tumor cells, *Biotechnic & Histochemistry* 78 (2003) 157–169.
- [57] [a] E.S. Van Amersfoort, J.A.G. Van Strijp, Evaluation of a flow cytometric fluorescence quenching assay of phagocytosis of sensitized sheep erythrocytes by polymorphonuclear leukocytes, *Cytometry* 17 (1994) 294–301;  
[b] L. Wu, L. Jiao, Q. Lu, E. Hao, Y. Zhou, Spectrofluorometric studies on the interaction between oxalix[6]arene-locked trizinc(II)porphyrins and crystal violet, *Spectrochimica Acta A* 73 (2009) 353–357.
- [58] K.E. Sapsford, L. Berti, I.L. Medintz, Materials for fluorescence resonance energy transfer analysis: beyond traditional donor–acceptor combinations, *Angewandte Chemie* 118 (2006) 4676–4704. *Angew. Chem. Int. Ed.* 45(2006) 4562–4588.
- [59] B. Huang, X. Zhou, Z. Xue, G. Wu, J. Du, D. Luo, T. Liu, J. Ru, X. Lu, Quenching of the electrochemiluminescence of Ru(bpy)<sub>3</sub><sup>2+</sup>/TPA by malachite green and crystal violet, *Talanta* 106 (2013) 174–180.
- [60] J.R. Masters, HeLa cells 50 years on: the good, the bad and the ugly, *Nature Reviews Cancer* 2 (2002) 315–319.

- [61] A. El-Sayed, S. Futaki, H. Harashima, Delivery of macromolecules using arginine-rich cell-penetrating peptides: ways to overcome endosomal entrapment, *AAPS Journal* 11 (2009) 13–22.
- [62] P. Midoux, M. Monsigny, Efficient gene transfer by histidylated polylysine/pDNA complexes, *Bioconjugate Chemistry* 10 (1999) 406–411.
- [63] A.J. Kowaltowski, J. Turin, G.L. Indig, A.E. Vercesi, Mitochondrial effects of triarylmethane dyes, *Journal of Bioenergetics and Biomembranes* 31 (1999) 581–590.
- [64] D. Magde, G.E. Rojas, P.G. Seybold, Solvent dependence of the fluorescence lifetime of xanthene dyes, *Photochemistry and Photobiology* 70 (1999) 737–744.
- [65] J.P. Richard, K. Melikov, E. Vives, C. Ramos, B. Verbeure, M.J. Gait, L.V. Chernomordik, B. Lebleu, Cell-penetrating peptides: a reevaluation of the mechanism of cellular uptake, *Journal of Biological Chemistry* 278 (2003) 585–590.
- [66] V. Barton, S.A. Ward, J. Chadwick, A. Hill, P.M. O'Neill, Rationale design of biotinylated antimalarial endoperoxides carbon centered radical prodrugs for application in proteomics, *Journal of Medicinal Chemistry* 53 (2010) 4555–4559.
- [67] H.-C. Peng, C.-C. Kang, M.-R. Liang, C.-Y. Chen, A. Demchenko, C.-T. Chen, P.-T. Chou, En route to white-light generation utilizing nanocomposites composed of ultrasmall CdSe nanodots and excited-state intramolecular proton transfer dyes, *ACS Applied Materials & Interfaces* 3 (2011) 1713–1720.
- [68] G.M. Sheldrick, A history of SHELX, *Acta Crystallographica A* 64 (2008) 112–122.